Cloud Physics Data

Thara Prabhakaran

Indian Institute of Tropical Meteorology
Pune, India

Air Data Probe (ADP) and AIMMS-20

Inertial probe

- Air speed
- Altitude
- Angle-of-attack
- Side-slip
- Ambient temperature
- Relative humidity.

WIND SPEED ACCURACY
Horizontal North and East Components:0.50 m/s (1.0 knot) @ 150 knot
Vertical:0.75 m/s (1.5 knots) @ 150 knot

TEMPERATURE Accuracy:0.30 C Resolution:0.01 C

RELATIVE HUMIDITY Accuracy:2.0% RH Resolution:0.1%RH

In situ measurements

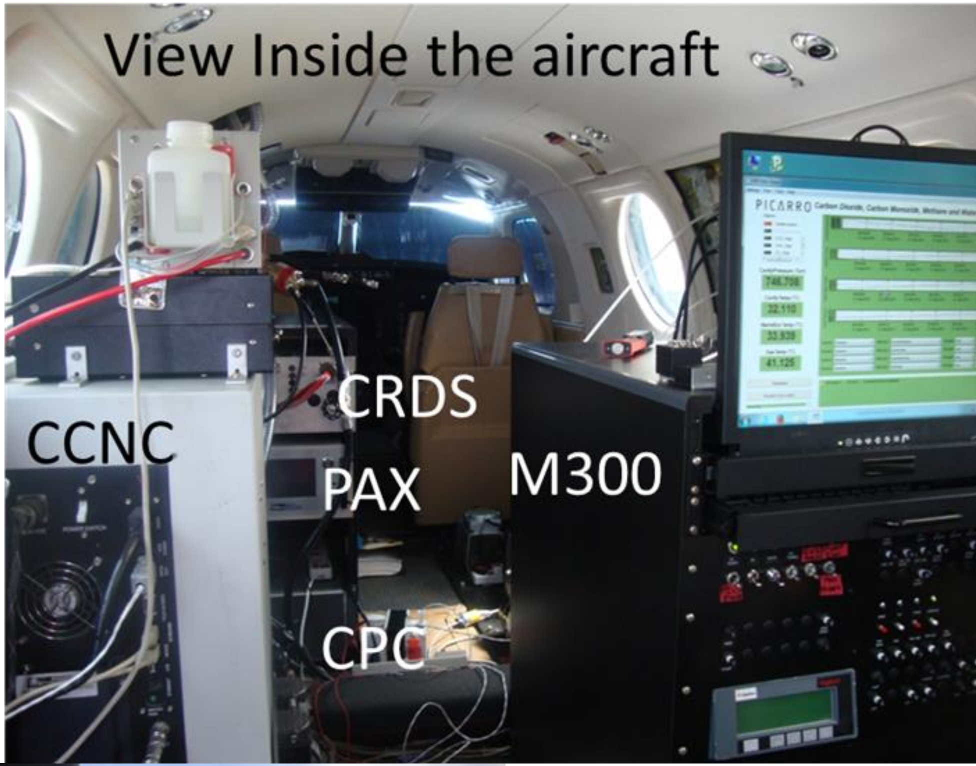

Cloud Aerosol Interaction and Precipitation Enhancement Experiment

CAIPEEX

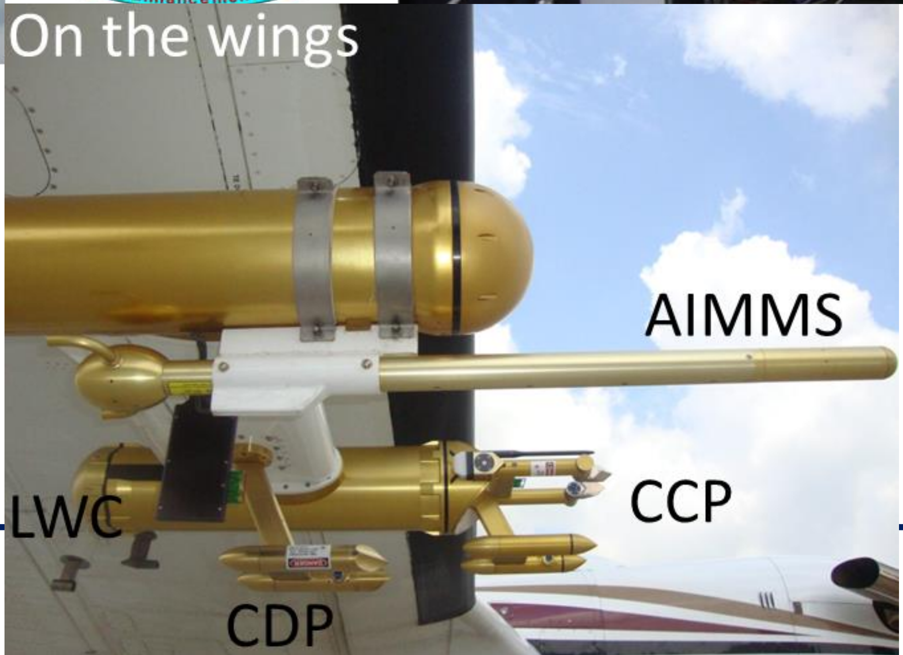

Indian Institute of Tropical Meteorology Pune

Cloud and ice particle measurements in clouds

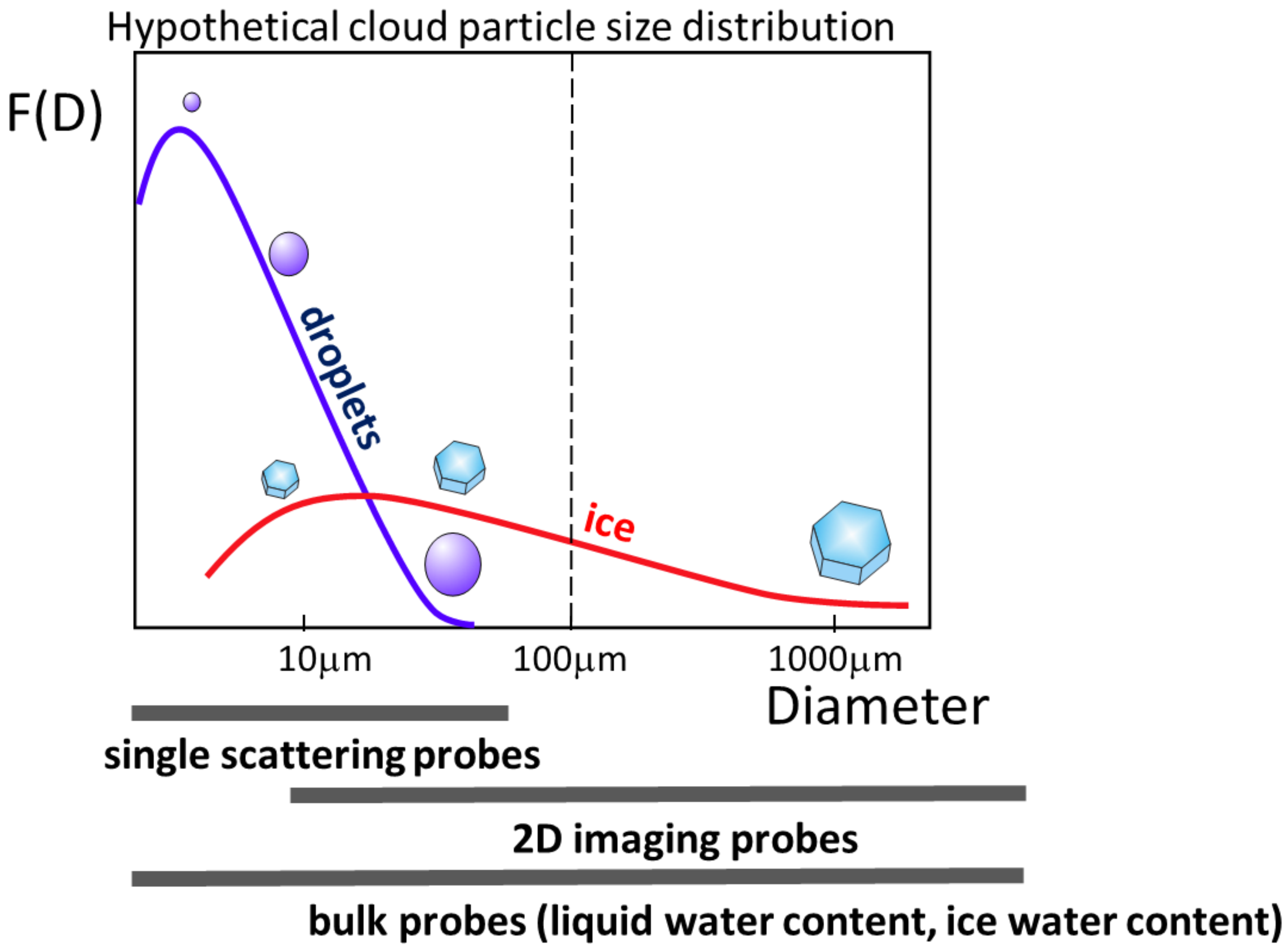

Sample of instruments used to address cloud physics

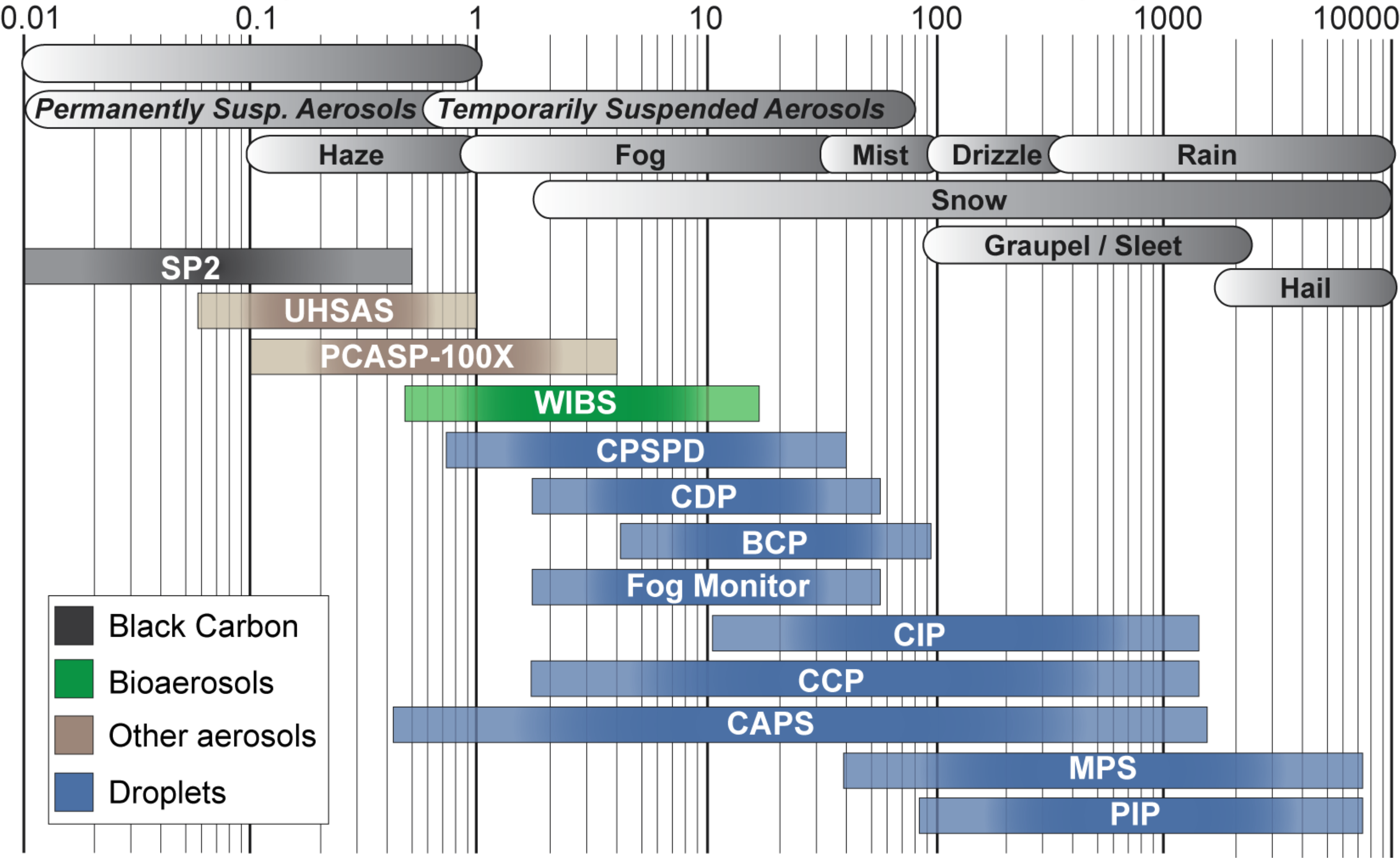

Source: DMT, Inc

Principles of operation of single particle scattering probes

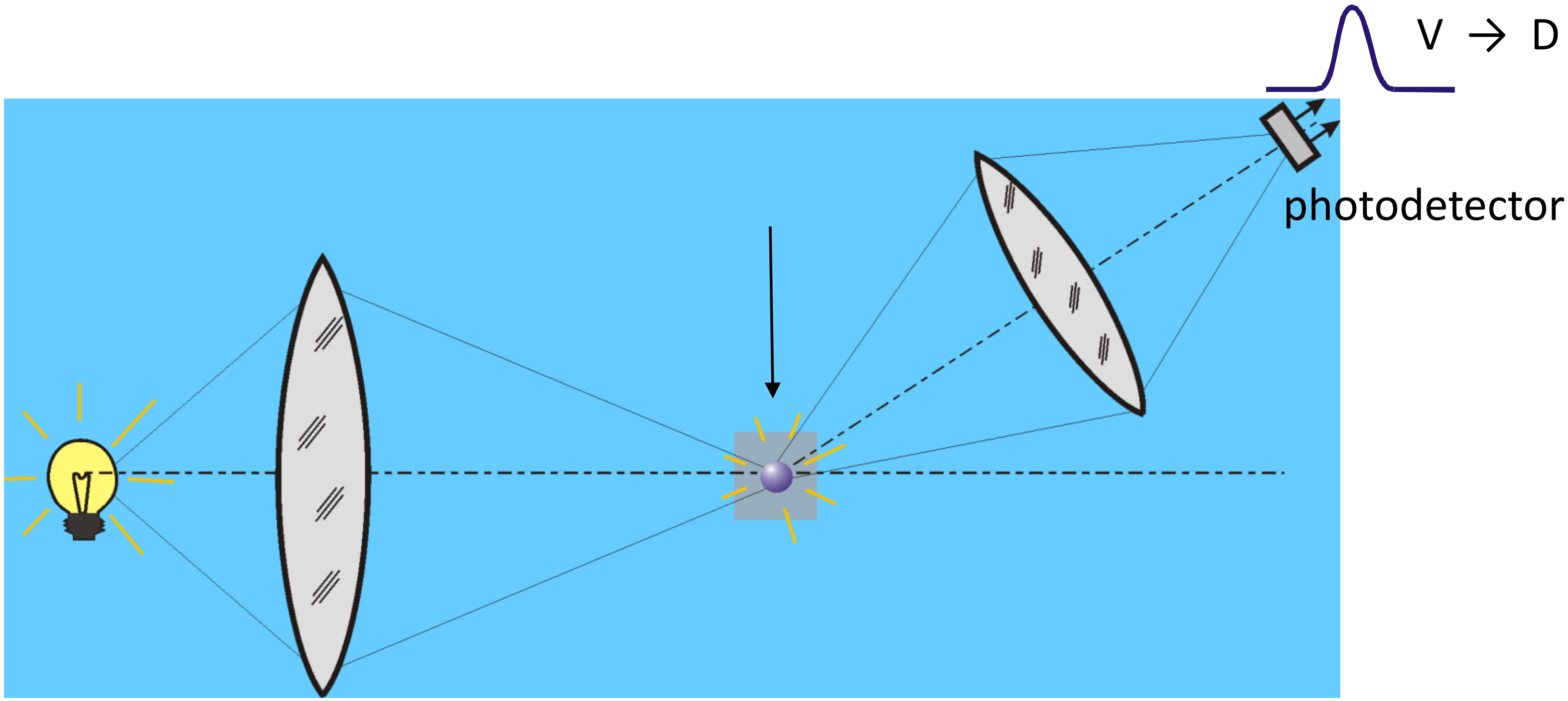

Particle size is determined based on the measurements of amount and properties **of light scattered** in a fixed aperture

Principle of operation of Optical Array Probes

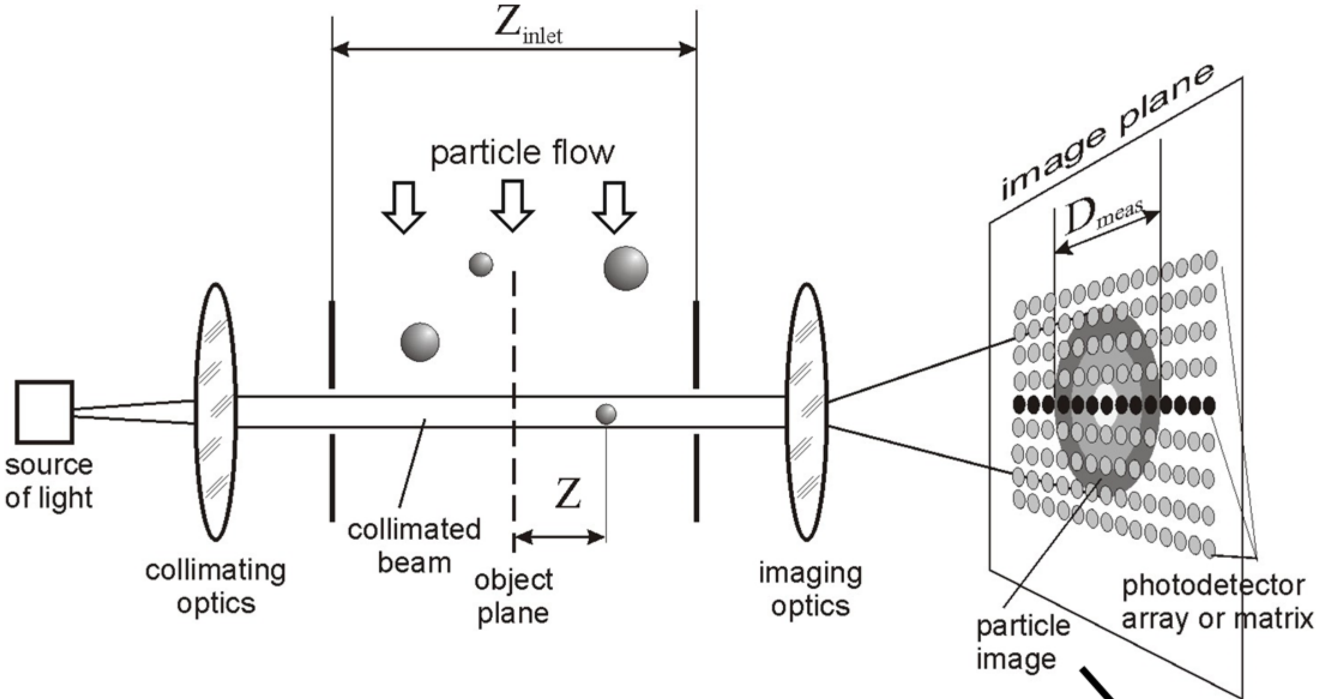

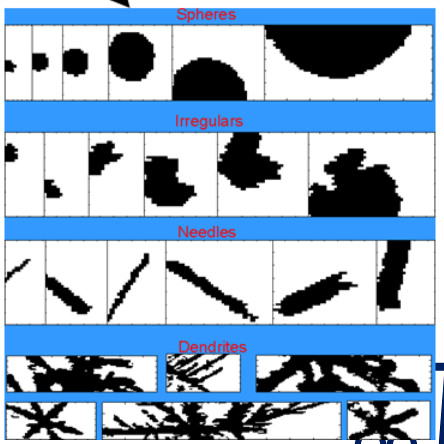

INDIAN INSTITUTE OF TROPICAL METEOROLOGY PUNE

Hot-wire probes: Total water content is calculated from the power required to maintain the heated wire at a constant temperature

LWC measurement

- Heated wire is exposed to the airstream
- Droplets impinge on the wire evaporate
- Cool- and lower the electrical resistance of the wire
- Power require to Keep the temperature of the wire constant

- Light scattering from drops also used

Shattering artifacts in the measurements
(DO not believe everything you see in the observations of ice)

Source: Alexei Korolev

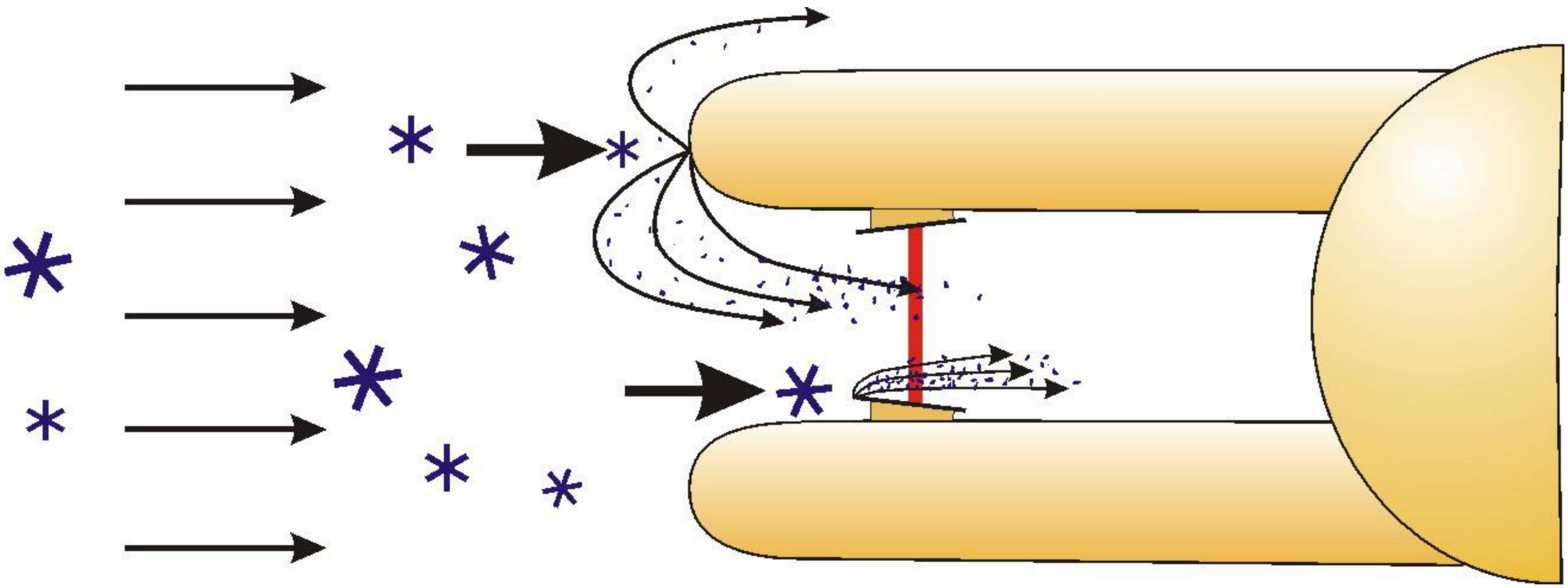

Effect of ice particle shattering on ice particle measurements

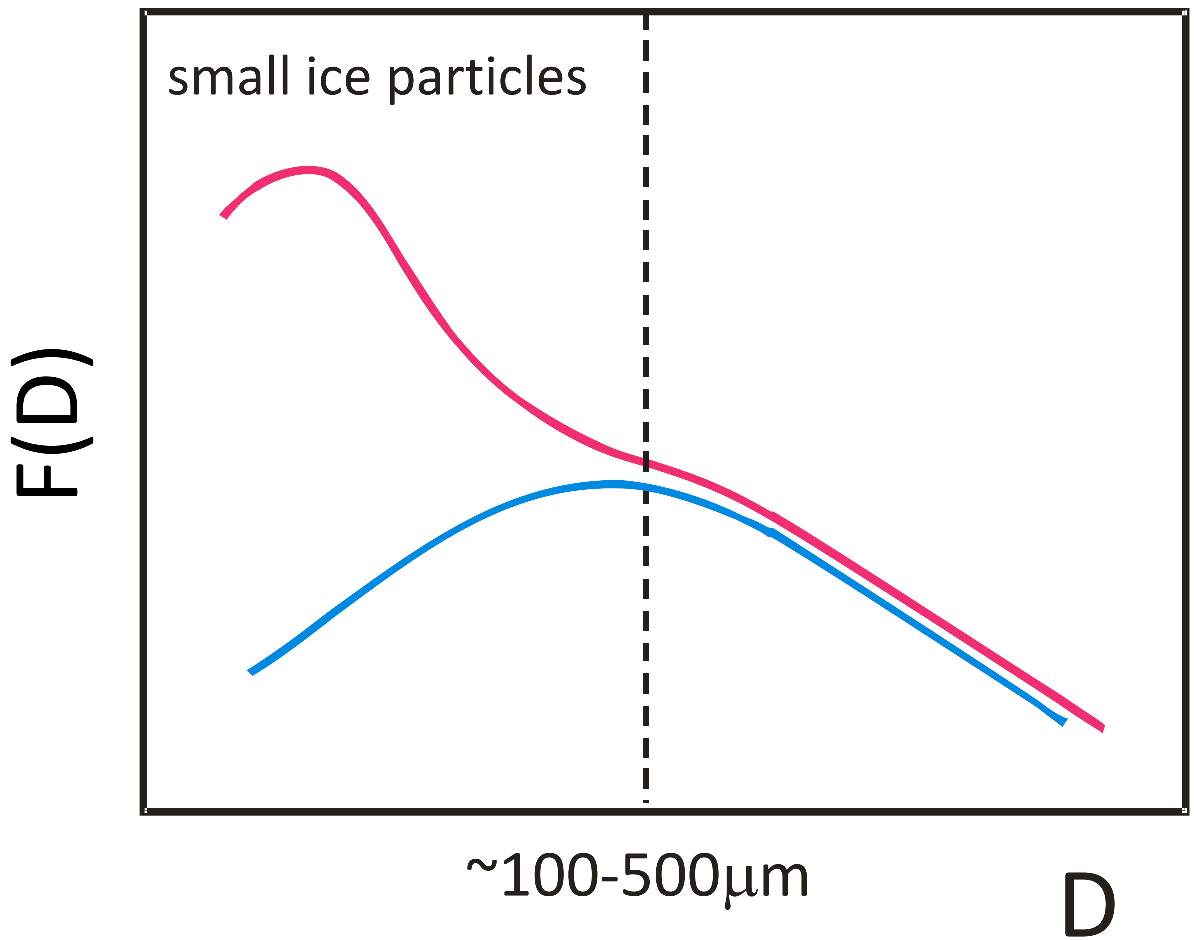

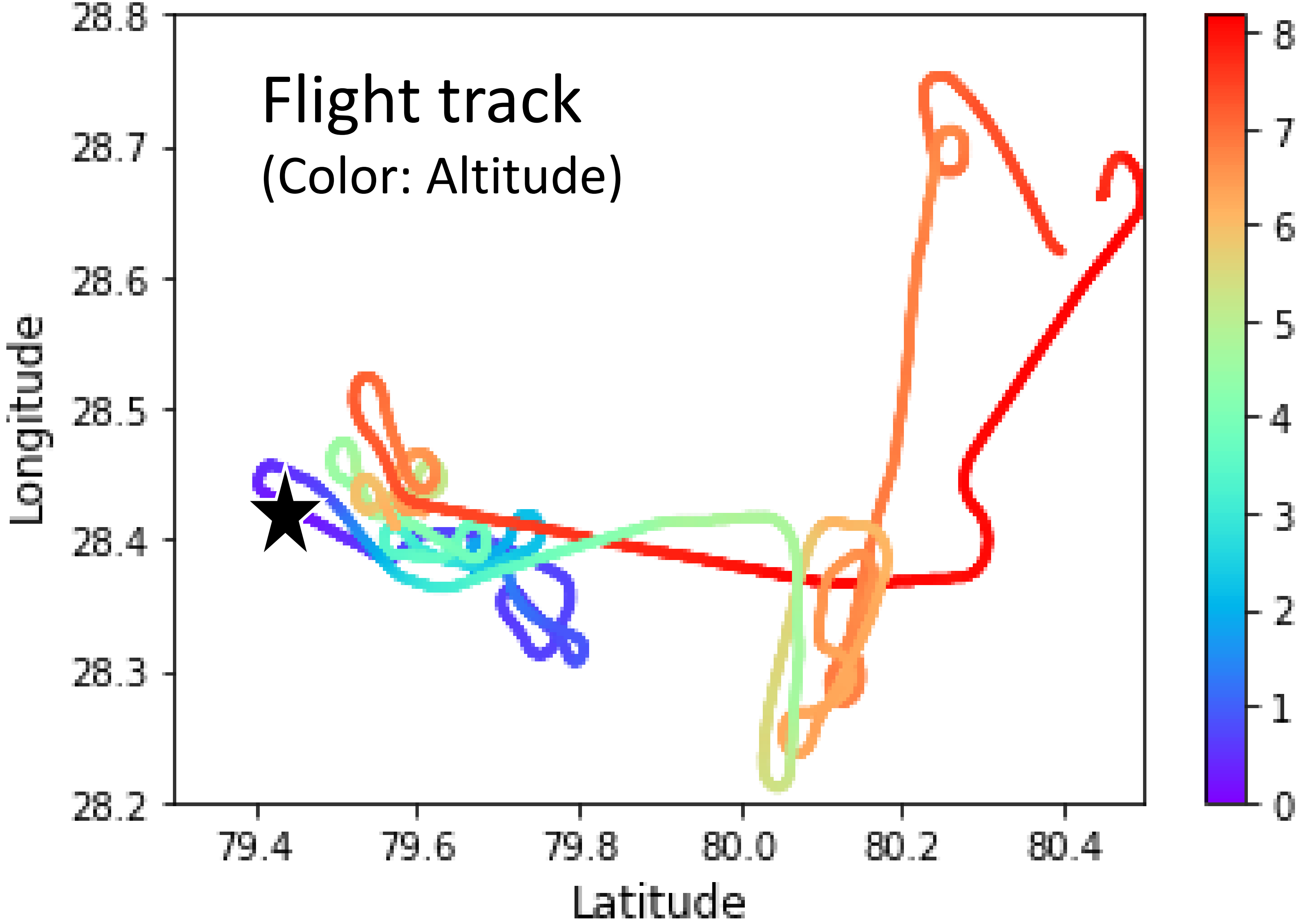

Flight track
(Color: Altitude)
28.8
28.7
28.6
28.5
28.4
28.3
28.2
Longitude
79.4
79.6
79.8
80.0
80.2
80.4
Latitude
8
7
6
5
4
3
2
1
0

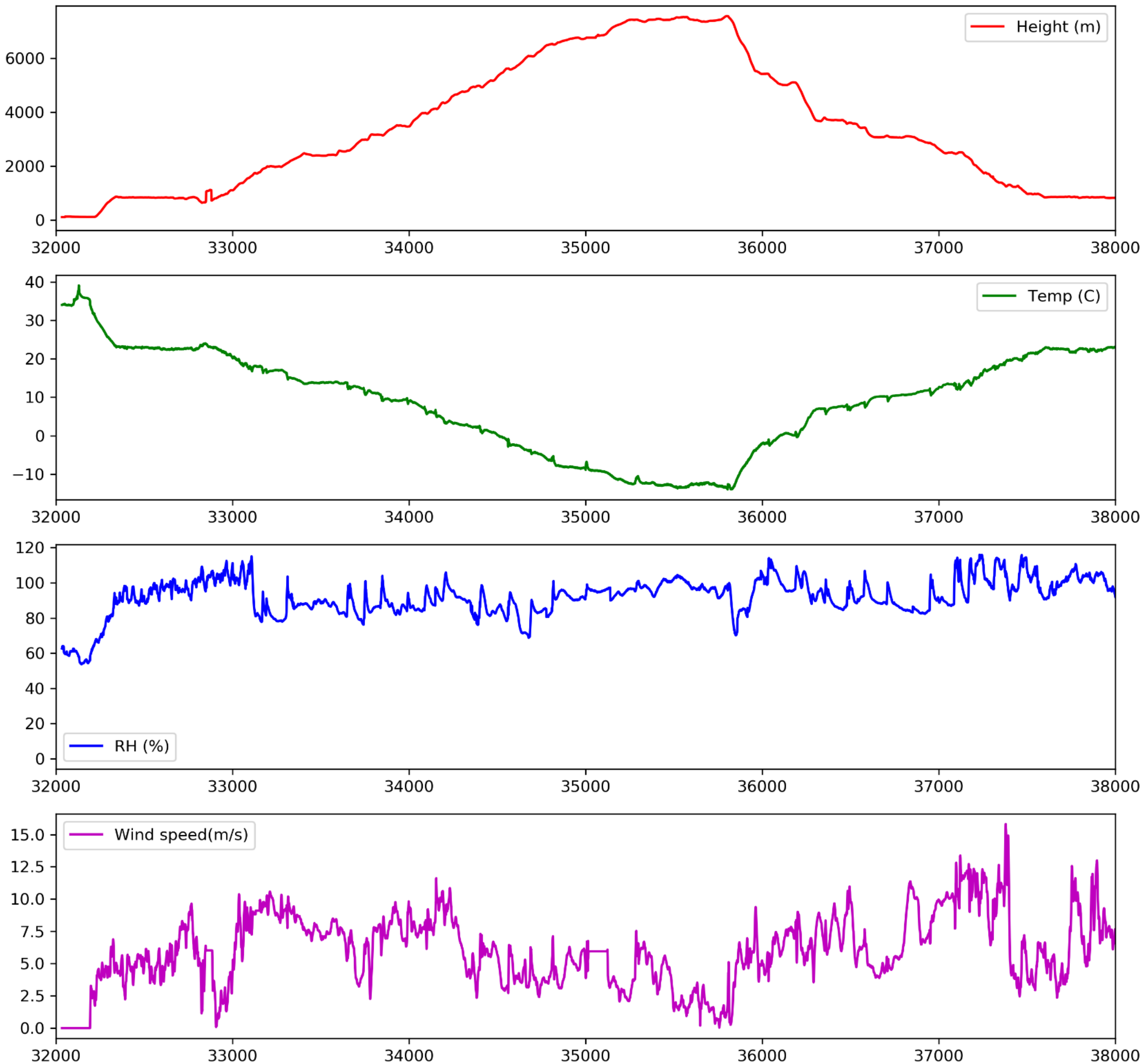

Height (m)
6000
4000
2000
0
32000
33000
34000
35000
36000
37000
38000
Temp (C)
40
30
20
10
0
−10
RH (%)
120
100
80
60
40
20
Wind speed(m/s)
15.0
12.5
10.0
7.5
5.0
2.5
0.0

Vertical variation of Aerosol and Cloud droplet number concentration

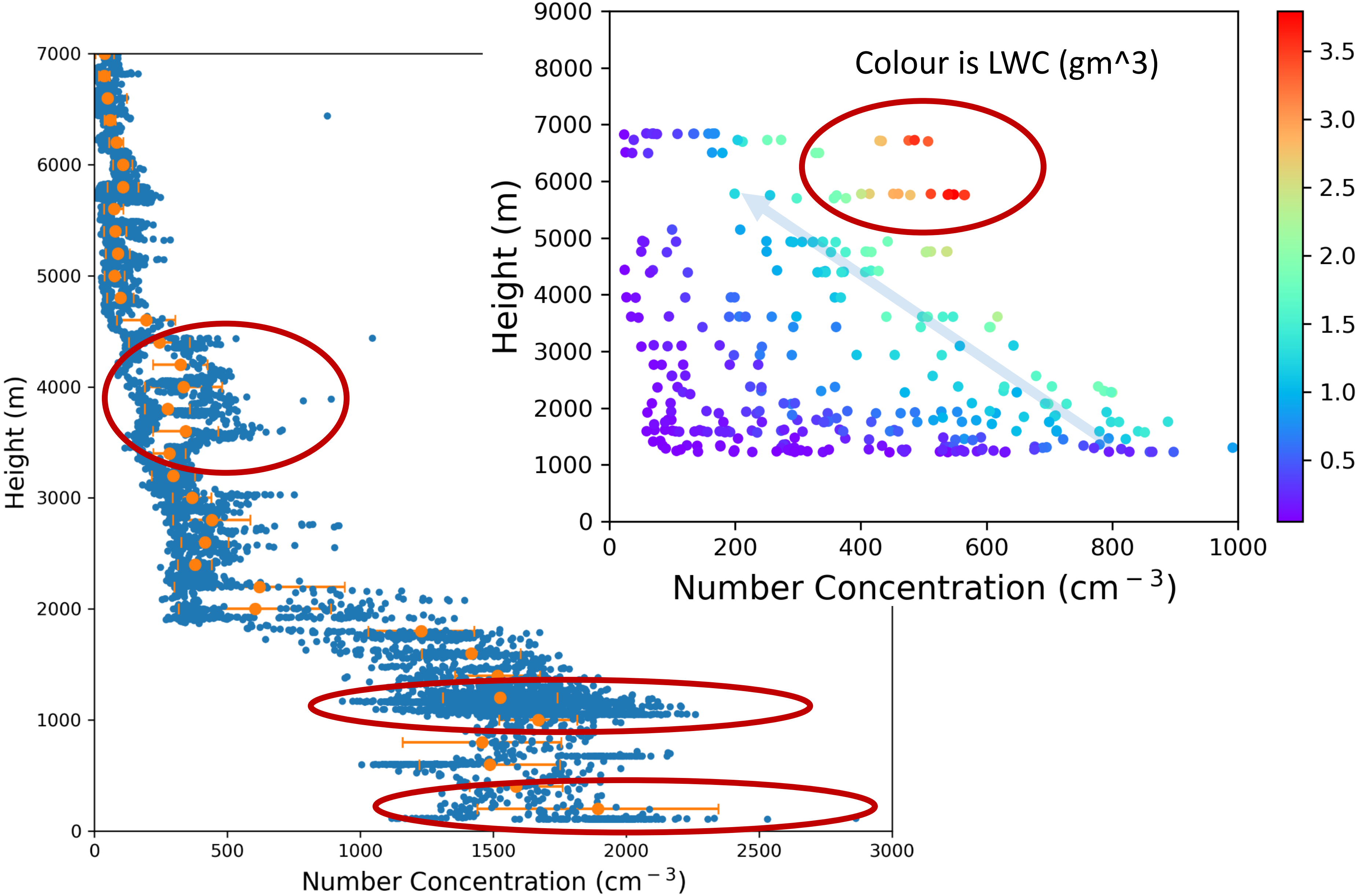

Liquid water content in Deep convective cloud

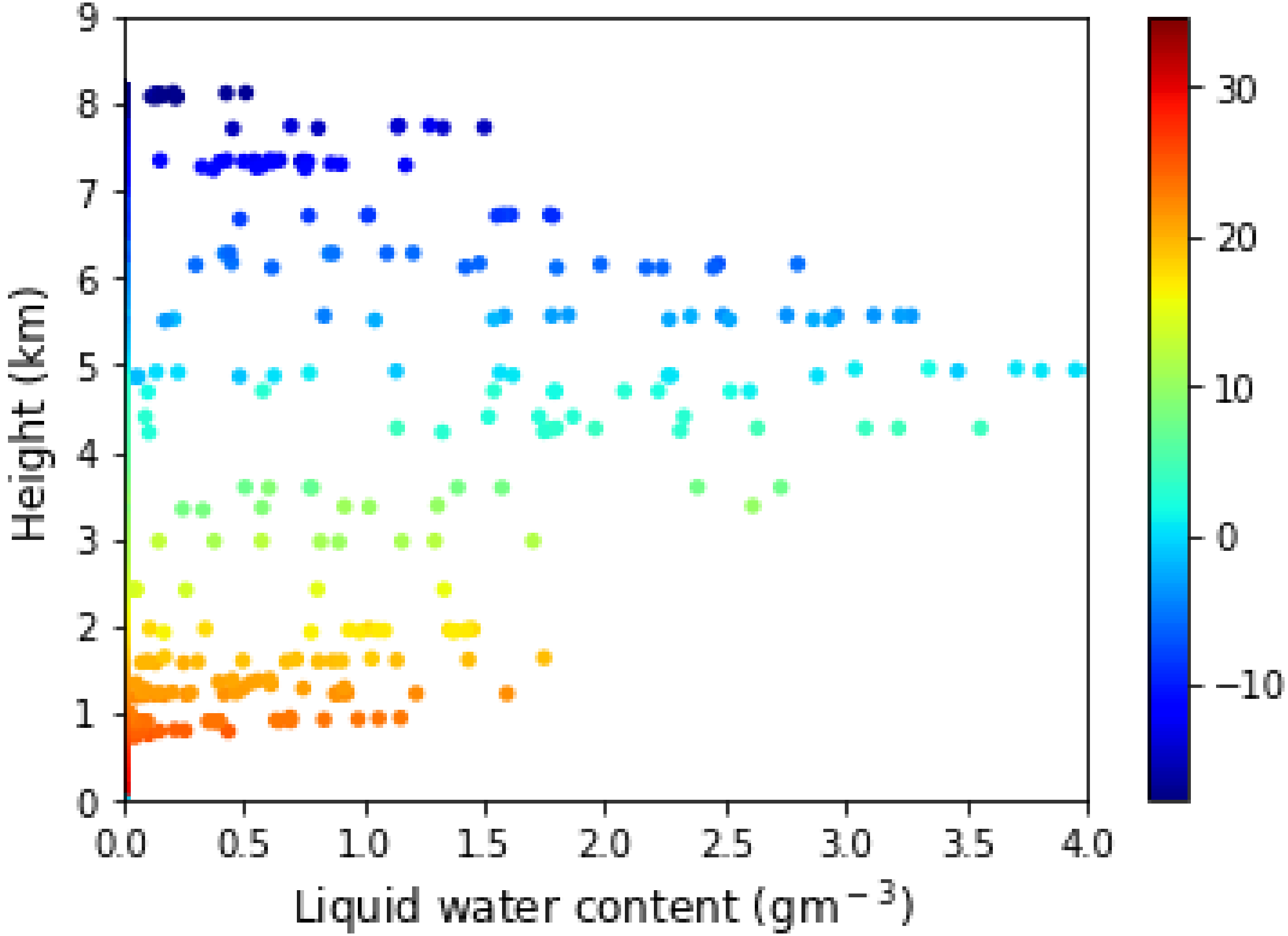

$$W \sim N\,\bar{r}^3 = \int f(r) r^3 dr$$ water content (3rd moment)

Effective radius in Deep convective cloud

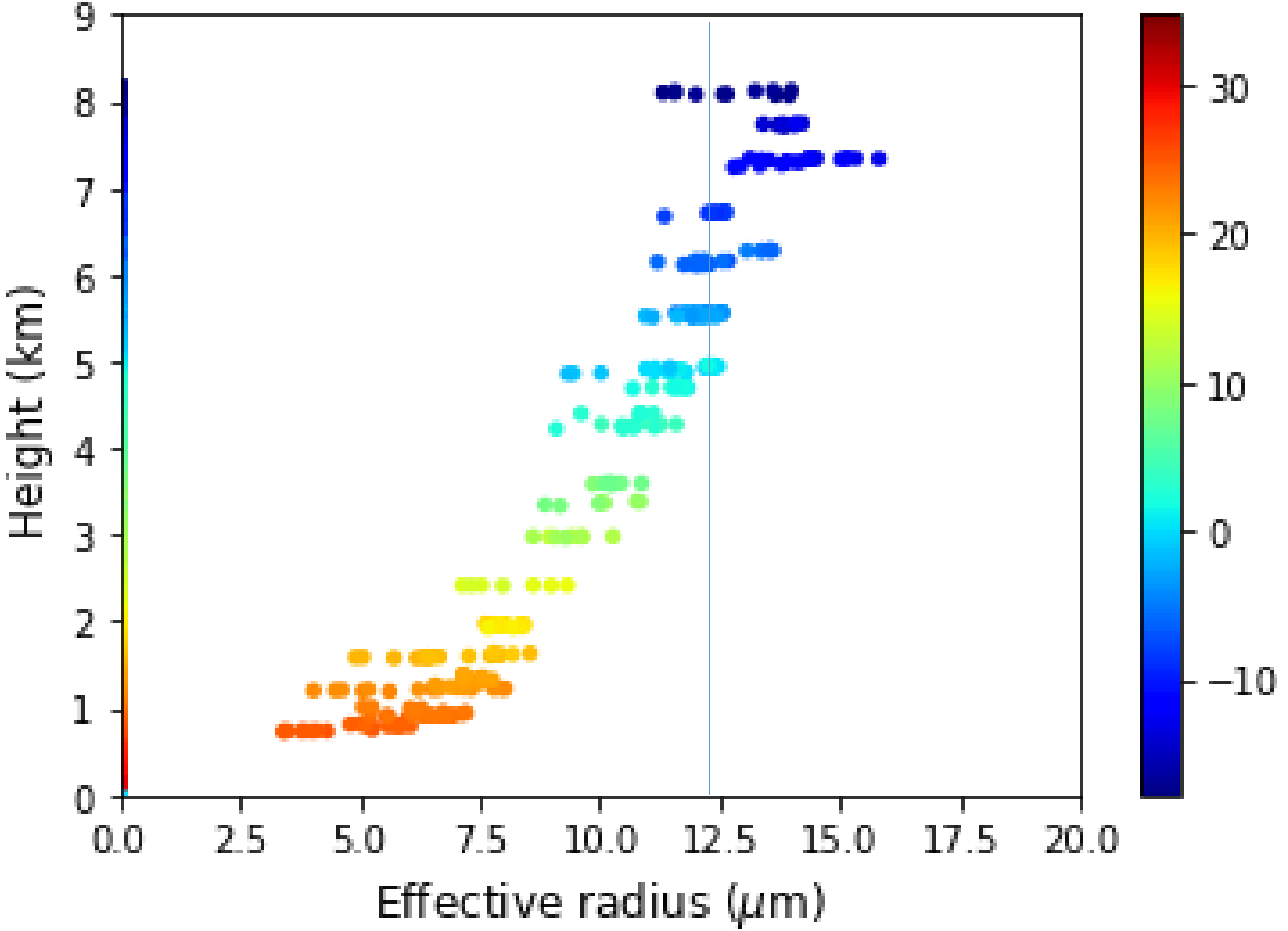

$$r_{eff} = \int f(r) r^3 dr / \int f(r) r^2 dr$$

Effective radius, Number concentration, Liquid water content

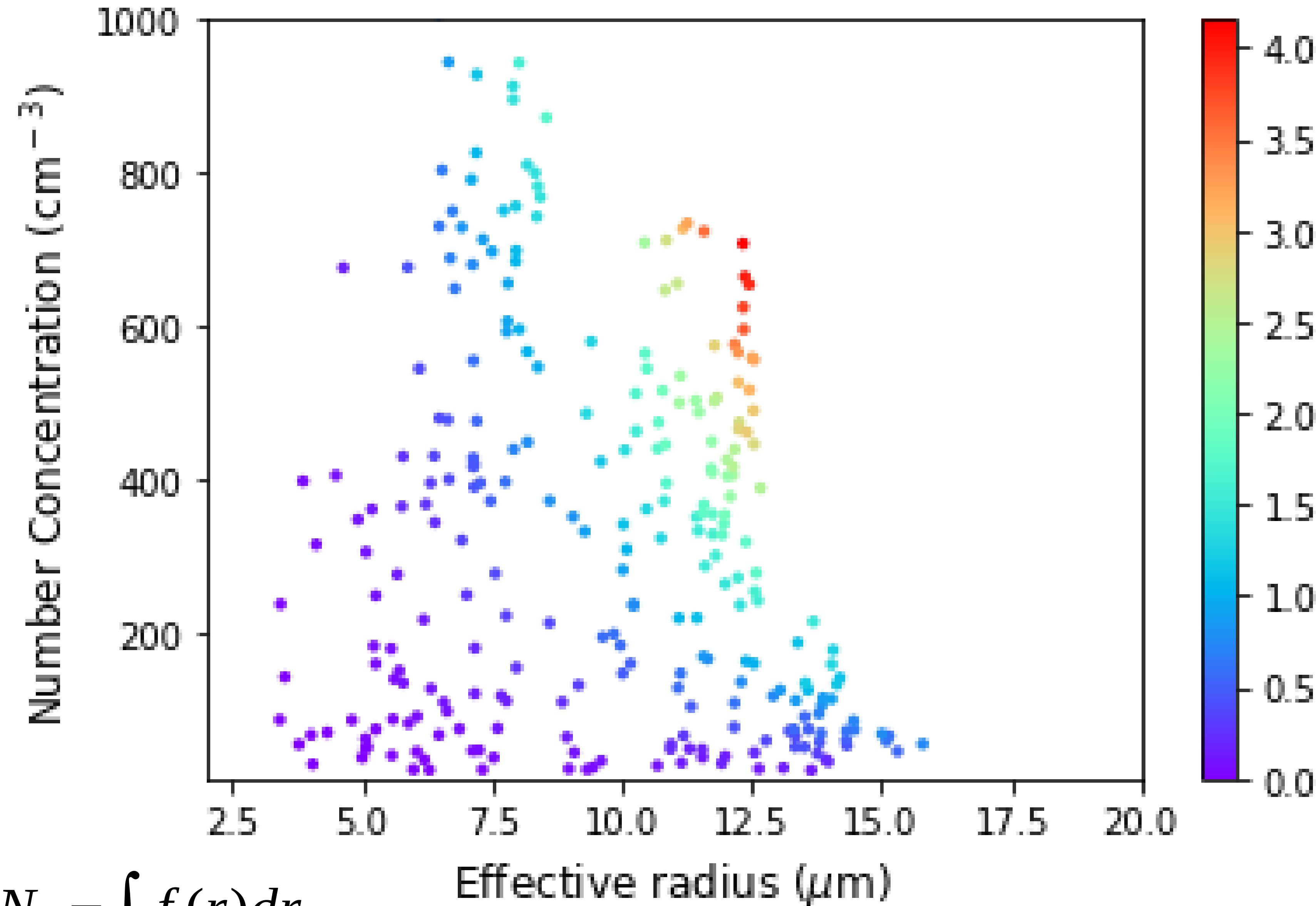

$$N = \int f(r)dr$$

Vertical velocity and number concentration

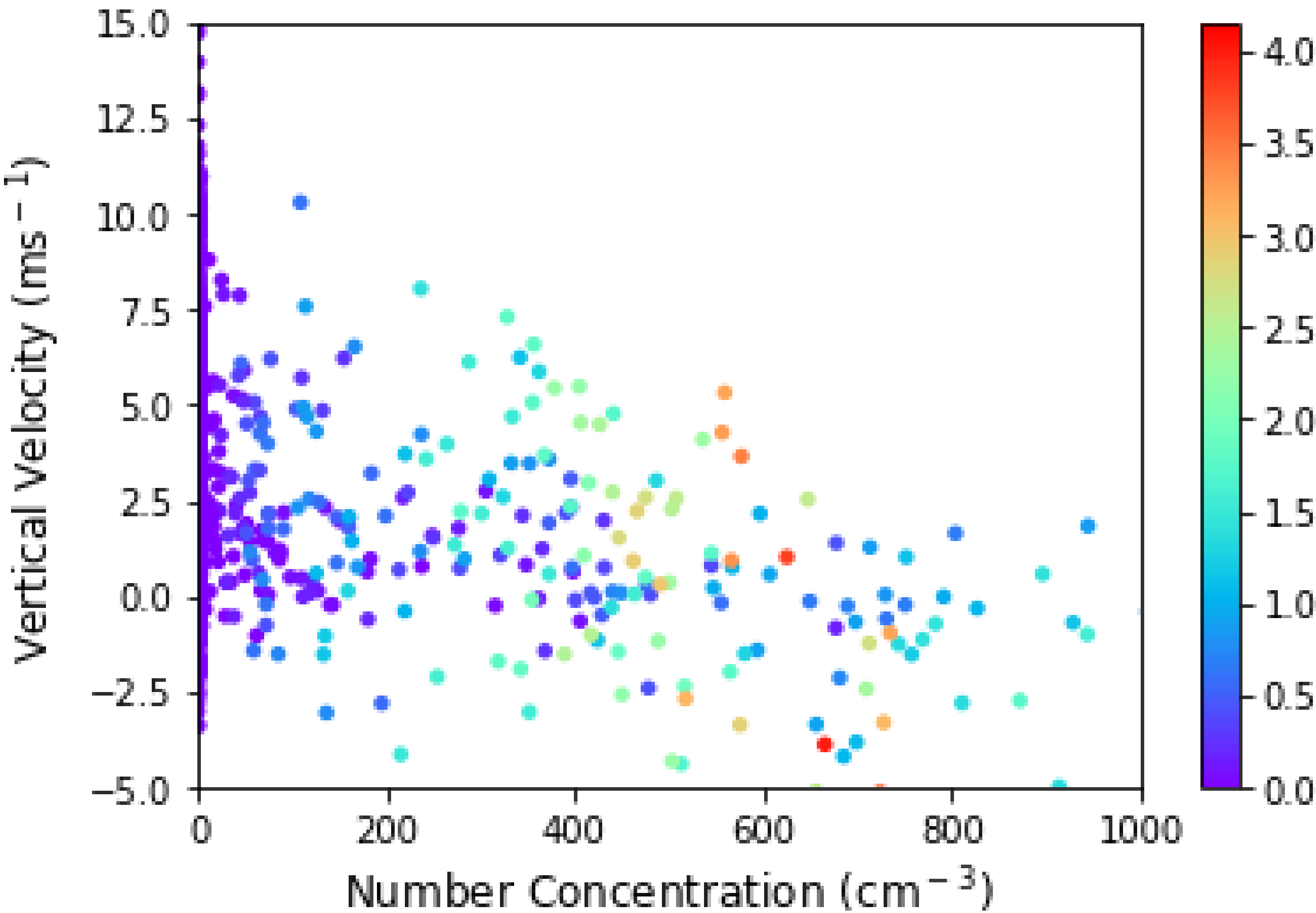

Vertical velocity and Effective radius

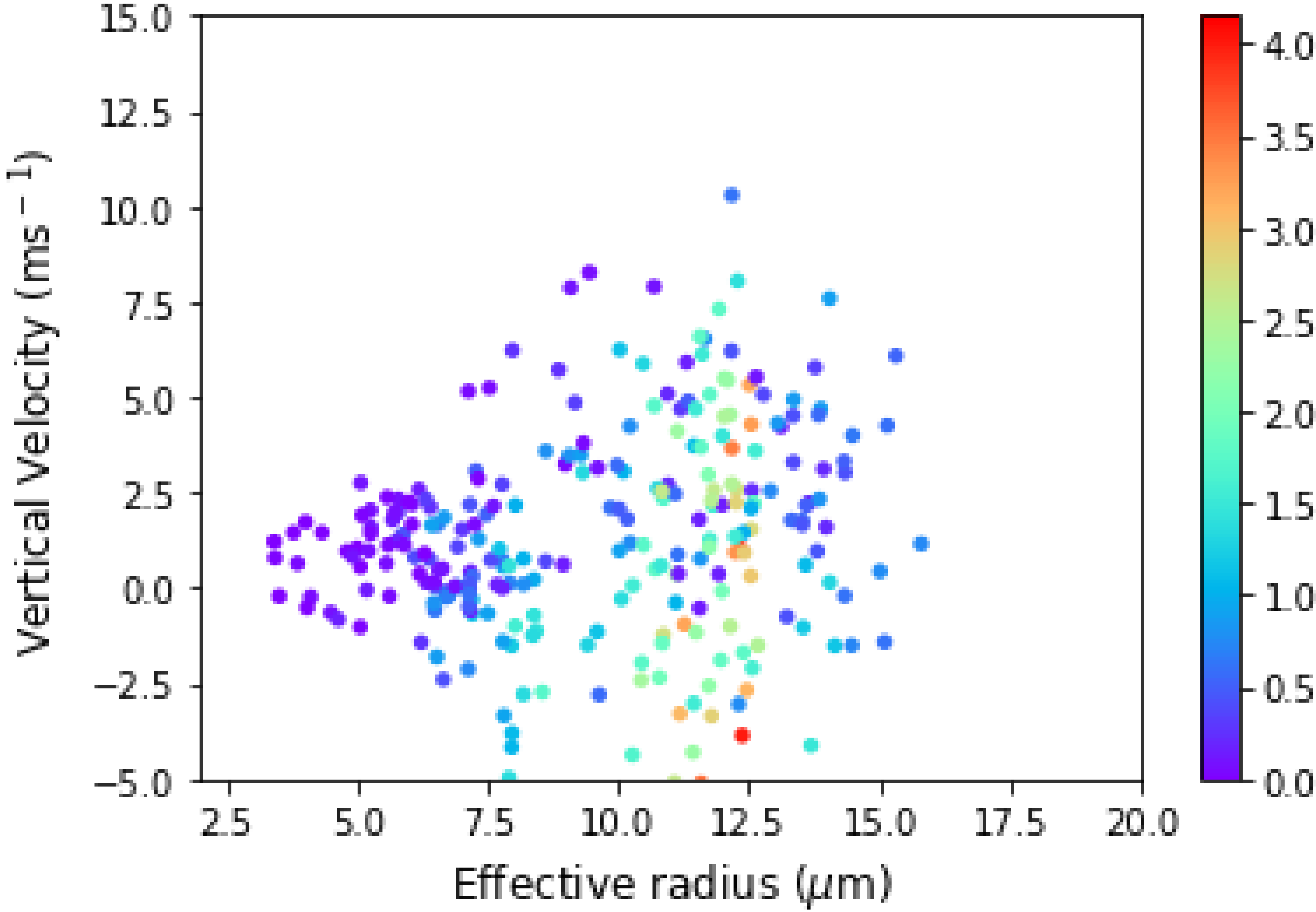

Aerosol number concentration

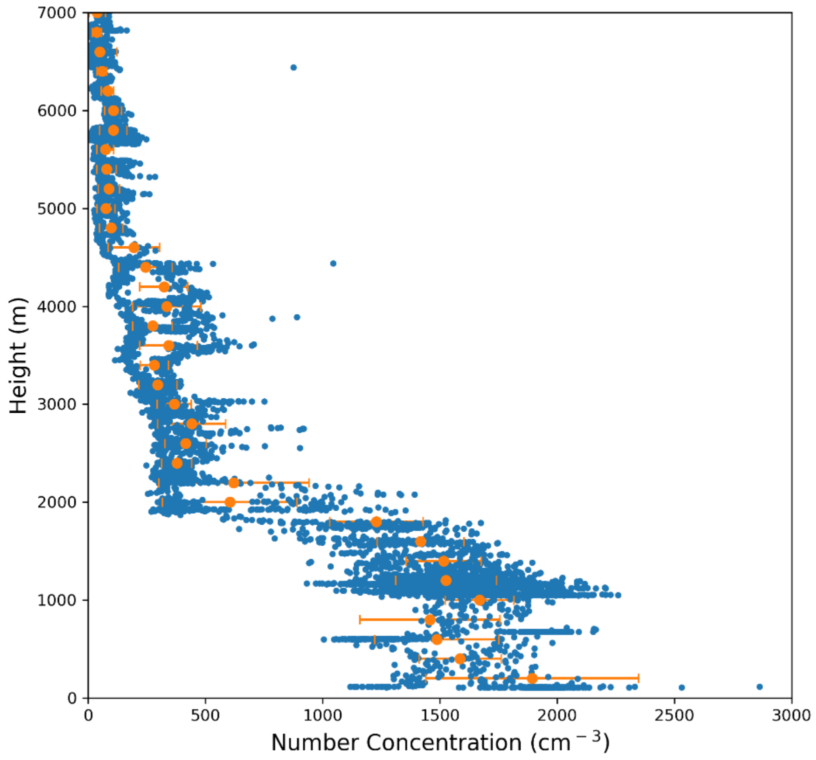

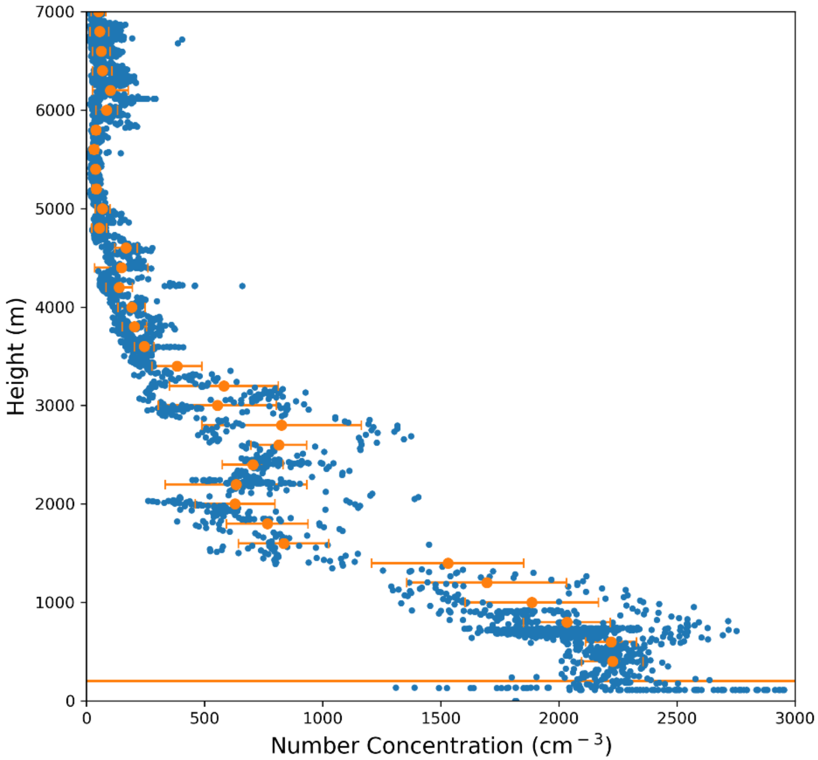

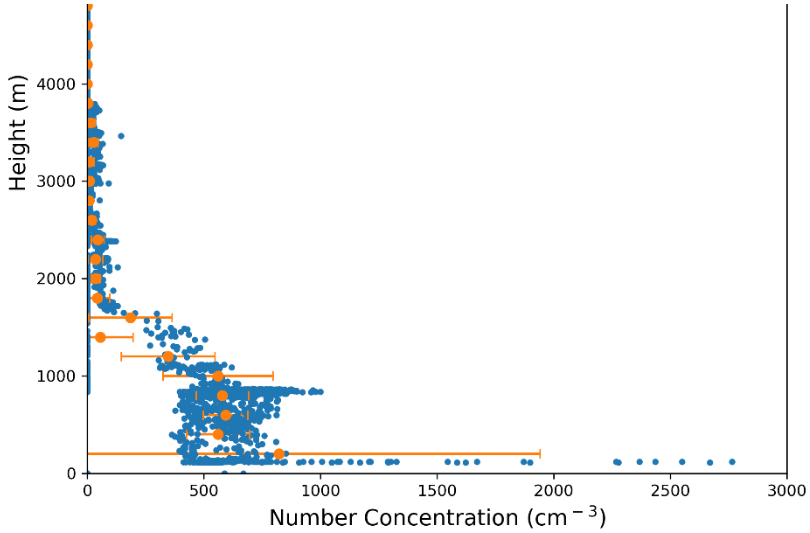

Cloud droplet number concentration

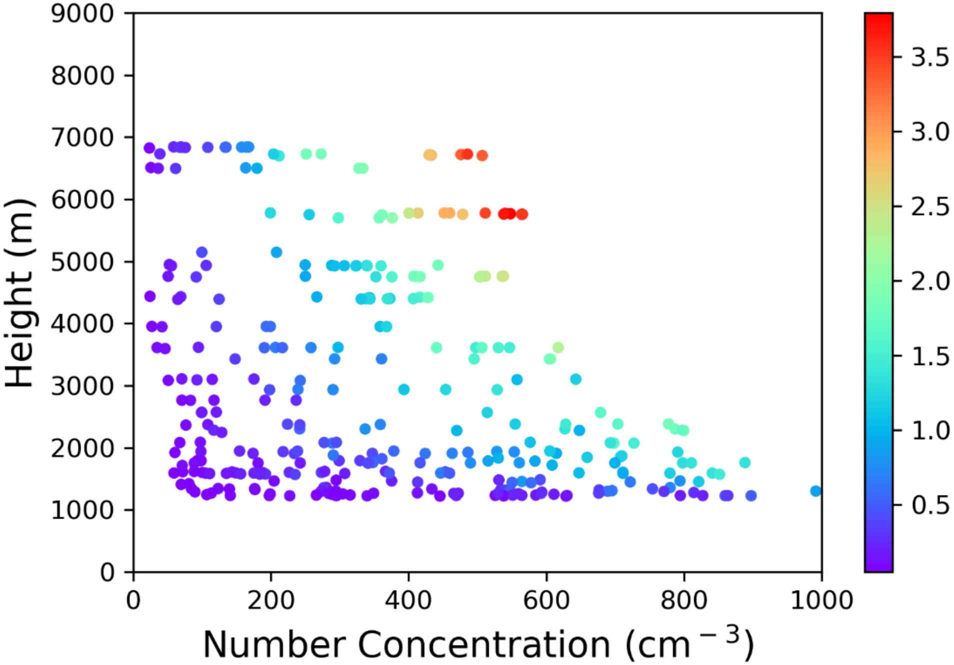

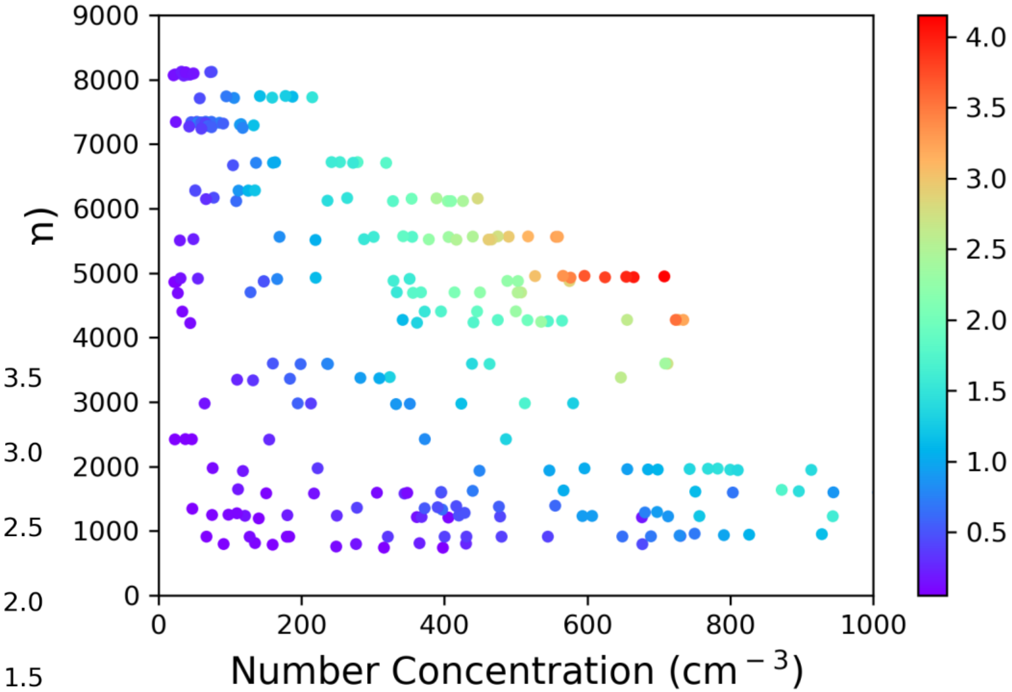

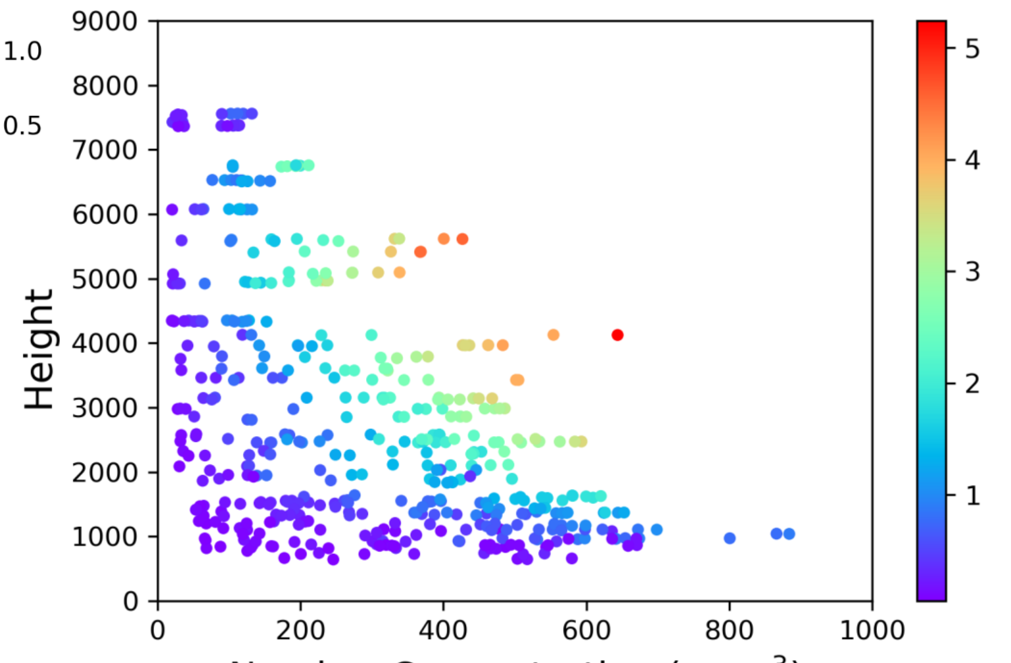

Cloud liquid water (CWC) profile from in situ measurements

- Maximum Liquid water content at higher elevation
- High supercooled liquid water content

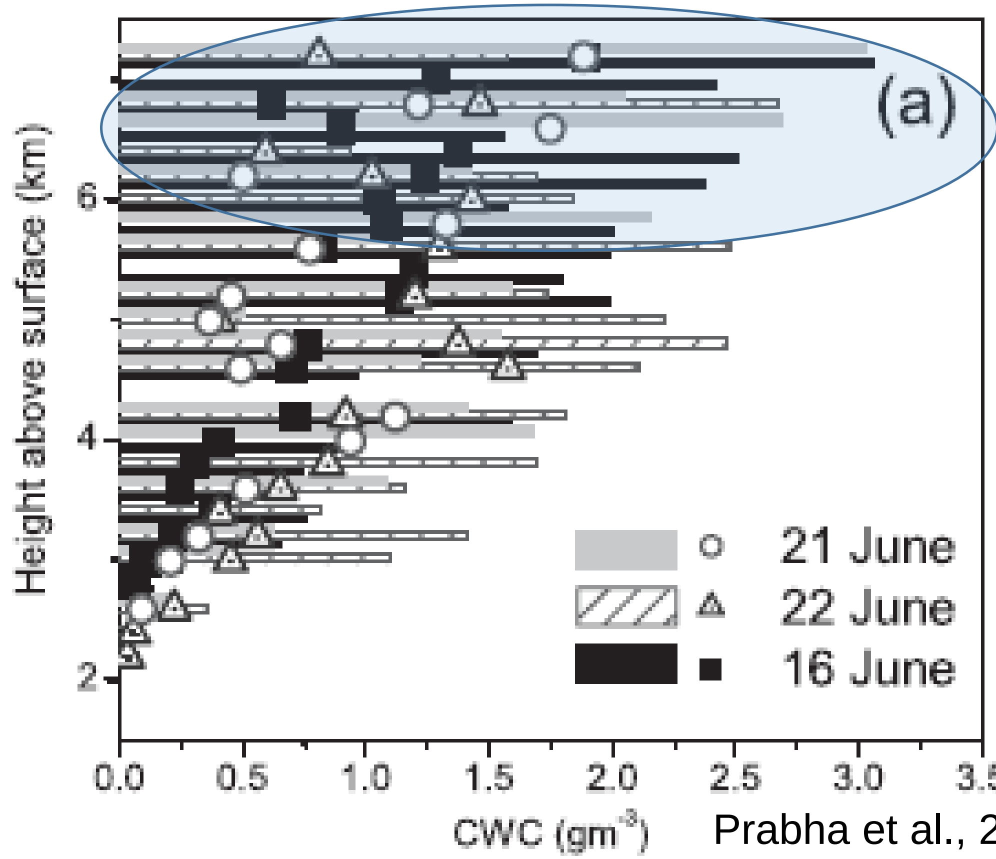

Prabha et al., 2011

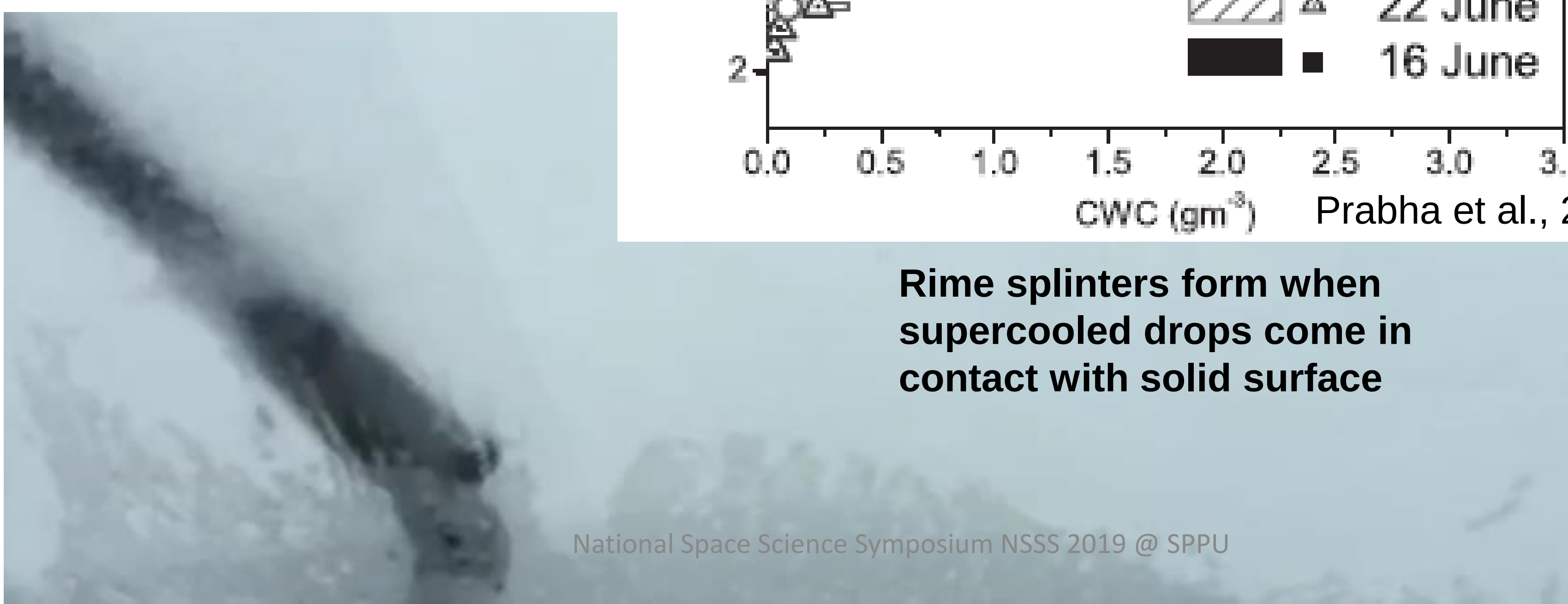

Rime splinters form when supercooled drops come in contact with solid surface

Identifying HM process from CAIPEEX observations

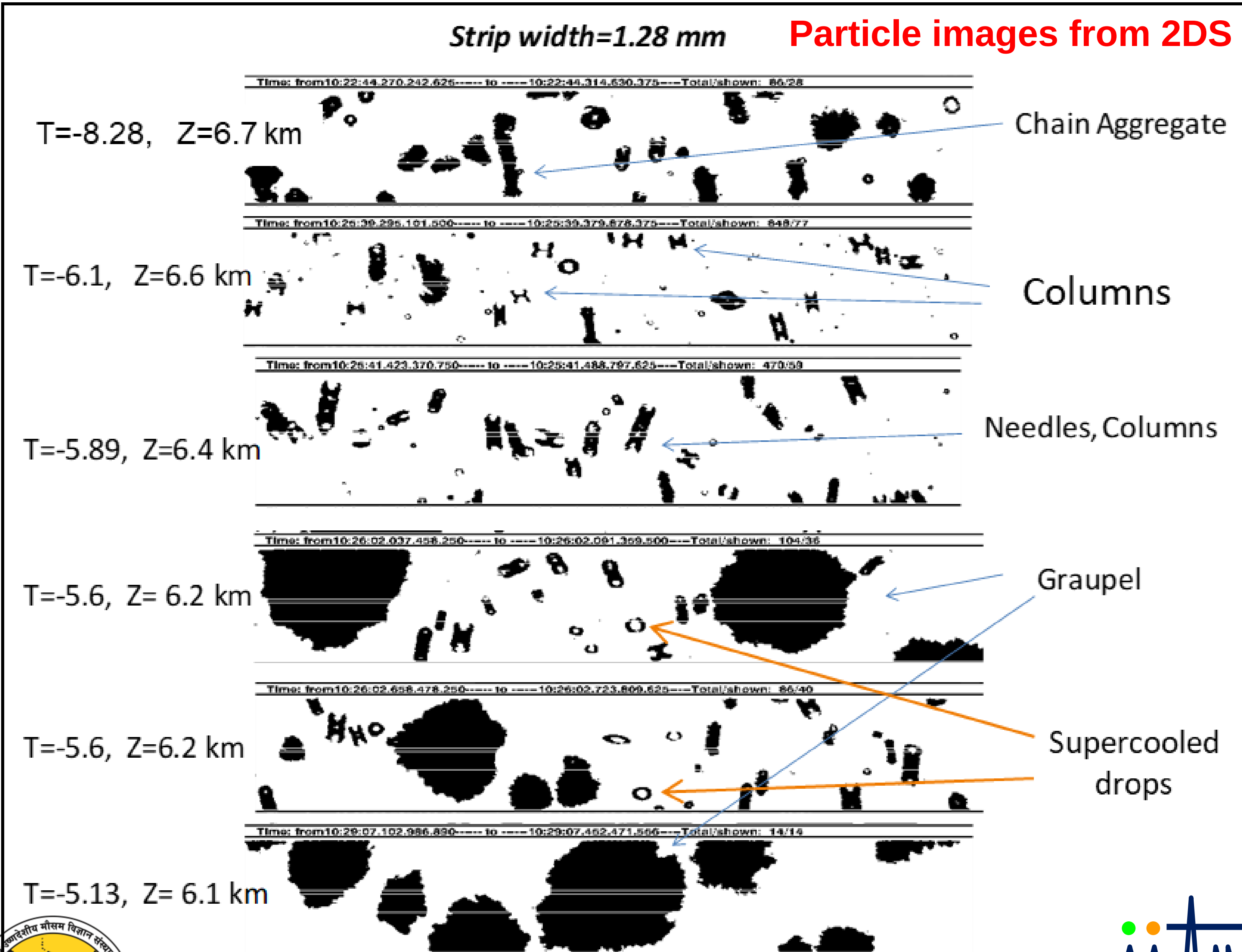

Gayatri K., S. Patade and T. V. Prabha. Aerosol cloud interaction in deep convective clouds over the Indian peninsula using Spectral (bin) Microphysics, 2017, *Journal of Atmospheric Science*,10.1175/JAS-D-17-0034.1

Forward scatter probe design

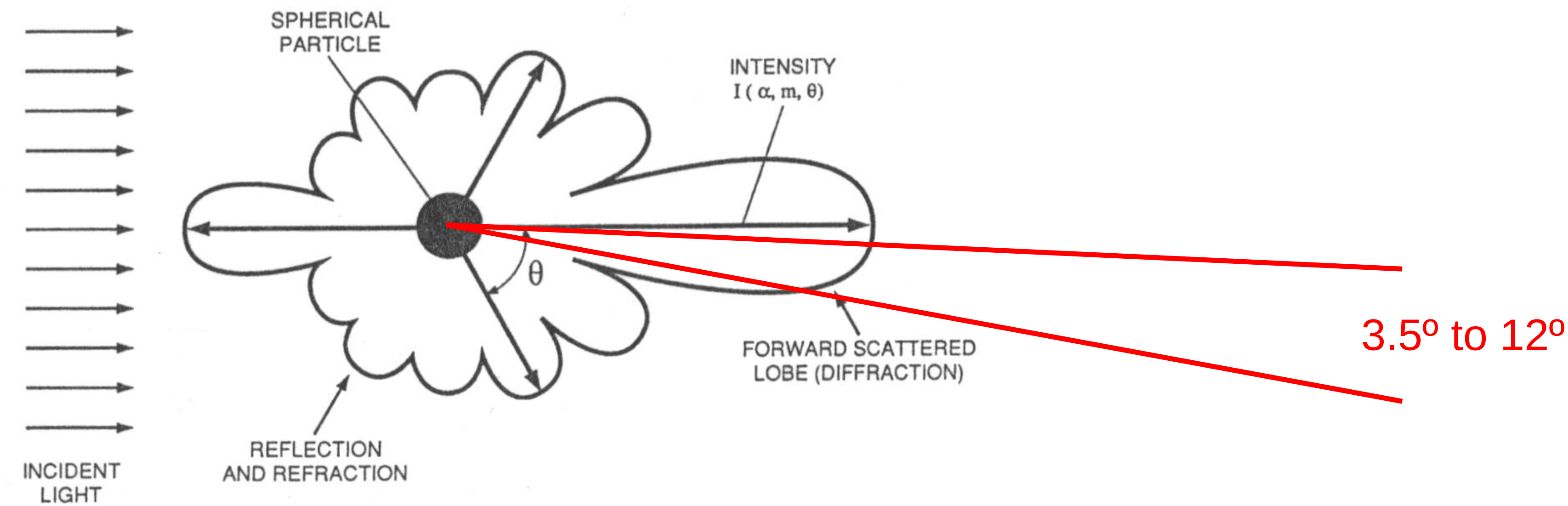

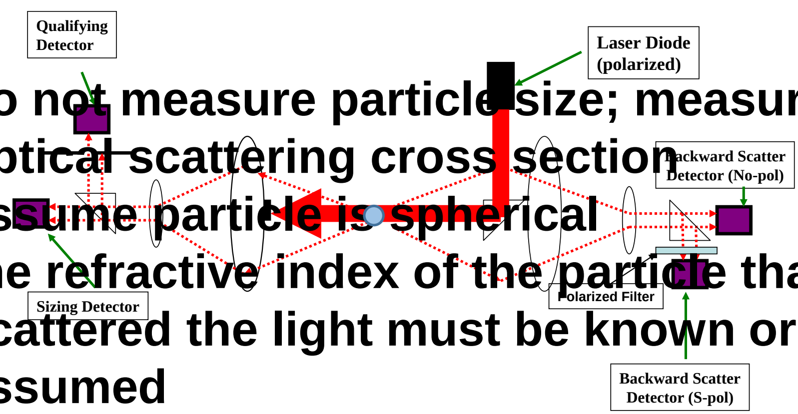

- do not measure particle size; measure optical scattering cross section
- assume particle is spherical
- the refractive index of the particle that scattered the light must be known or assumed
- assumes setup table based on calibration

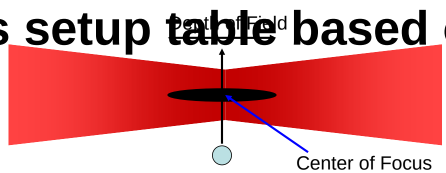

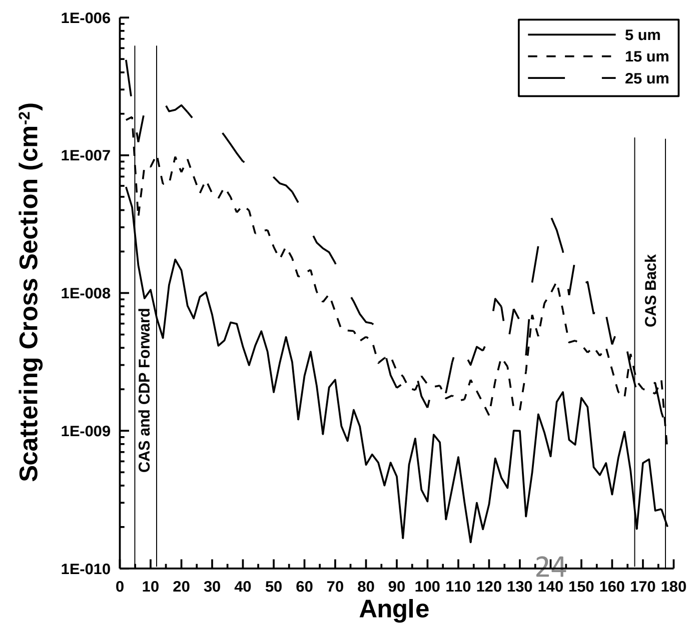

Optical array probe design

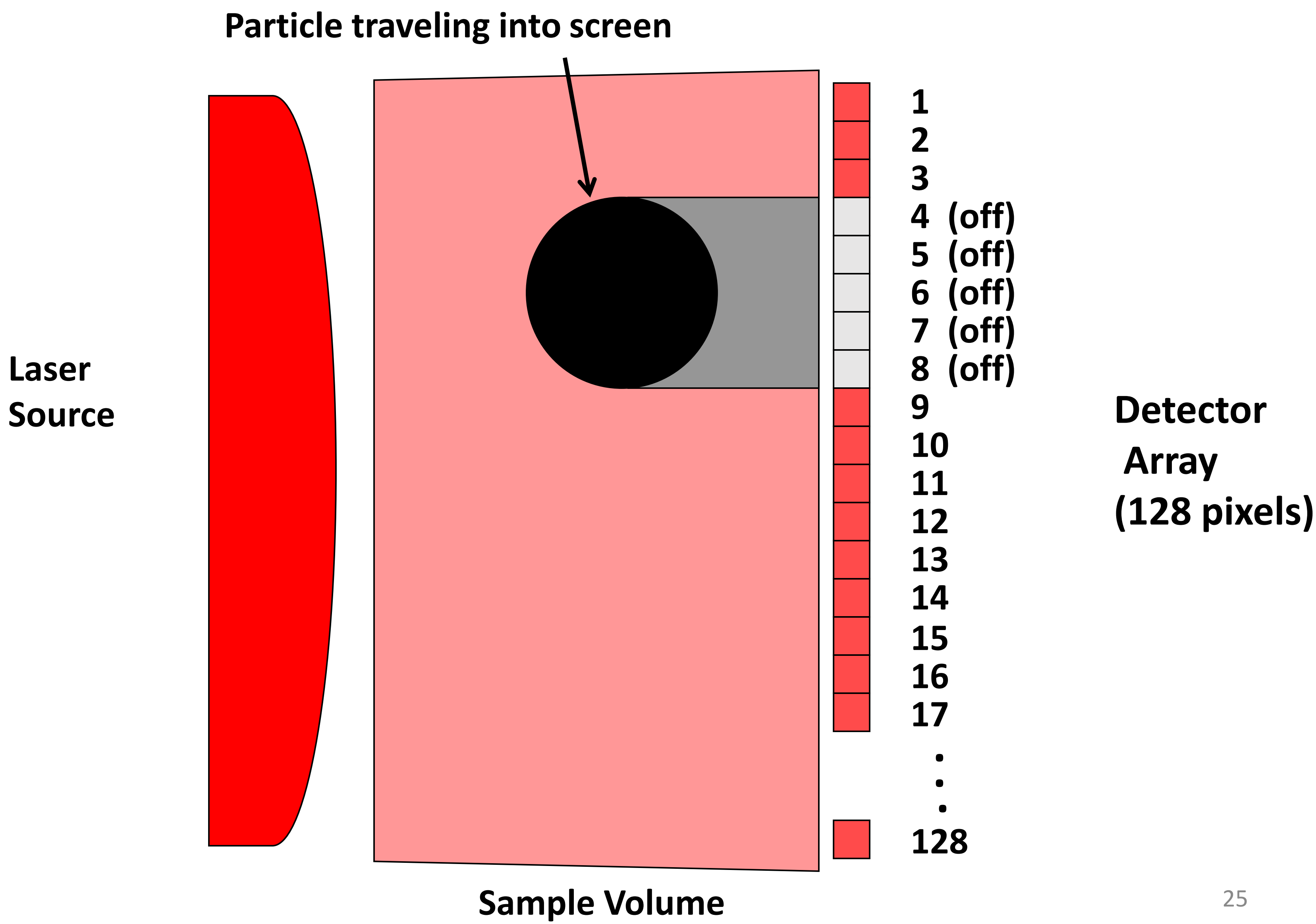

Common errors/limitations with forward scatter probes and OAPs

- errors associated with coincidence (more than one droplet in the measurement volume at one time)
- errors due to drift in calibration (need for frequent calibrations)
- errors due to beam attenuation and optical contamination (need for frequent cleaning)
- limited size range for the forward scatter probes (FSSP/CAS) in measurement of drizzle drops
- incomplete knowledge of the correct depth of field for the OAPs (CIP, PIP and 2DS) to size large hydrometeors
- uncertainty in merging of the droplet size ranges (FSSP/CAS with 2DS/CIP)
- errors due to droplet breakup and splash due to mechanical impact and interactions with the aerodynamic field with probe parts upstream of the sample area
- blurred or out of focus images produced by particles that pass the OAP system out of the object plane leading to erroneous particle sizing.


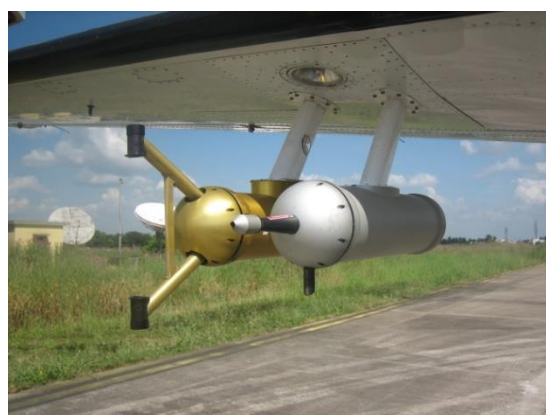


FSSP optical contamination

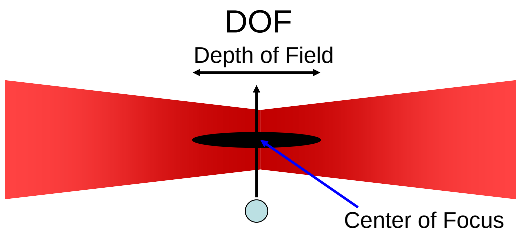

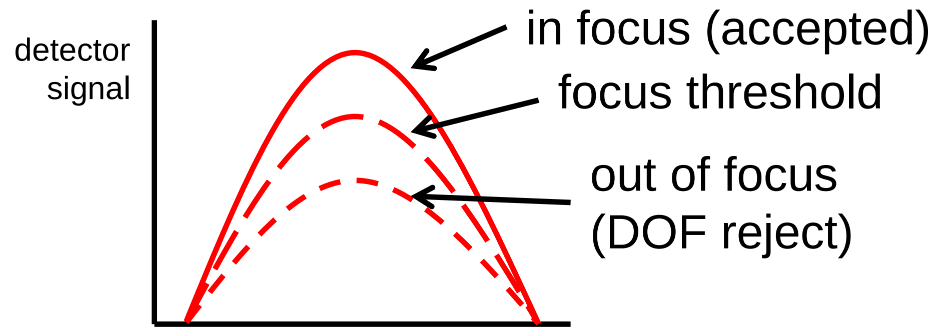

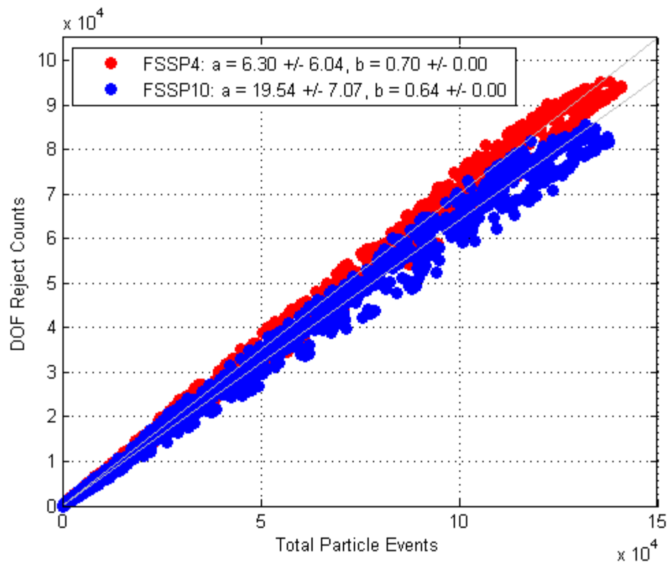

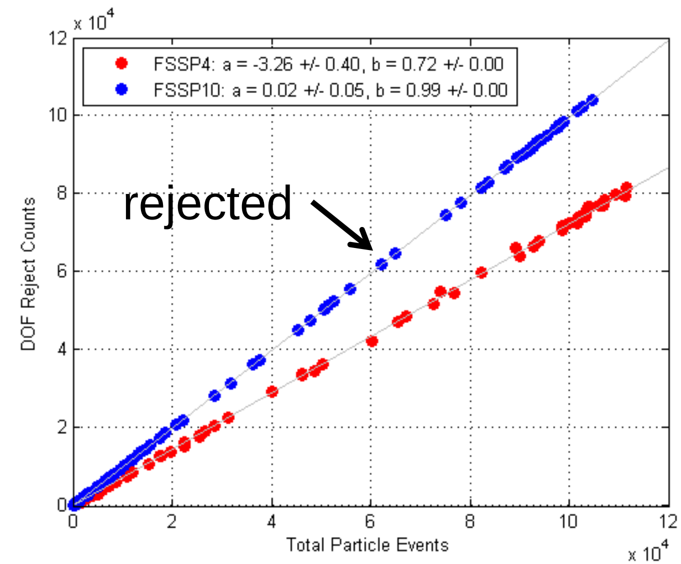

Plots of total particle events and rejected counts for arf11 (left) and arf17 (right). A ratio greater than 0.85 is unacceptable, i.e., FSSP10 data for arf11 are rejected.

Comparisons between FSSP LWC and hotwire LWC

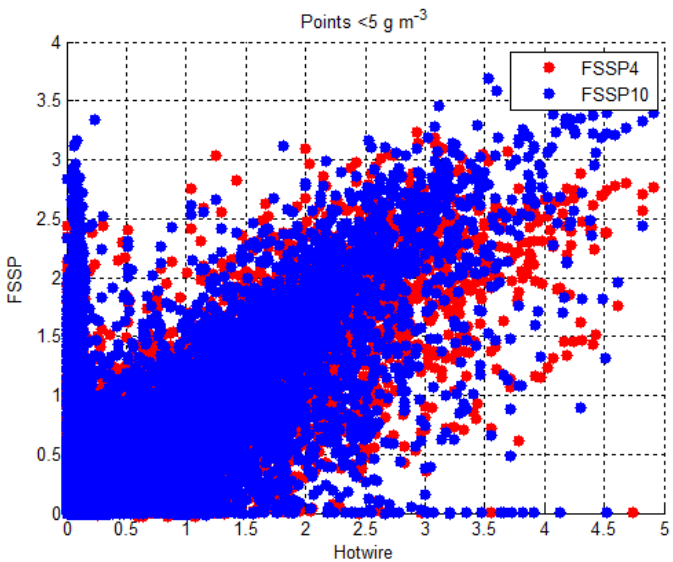

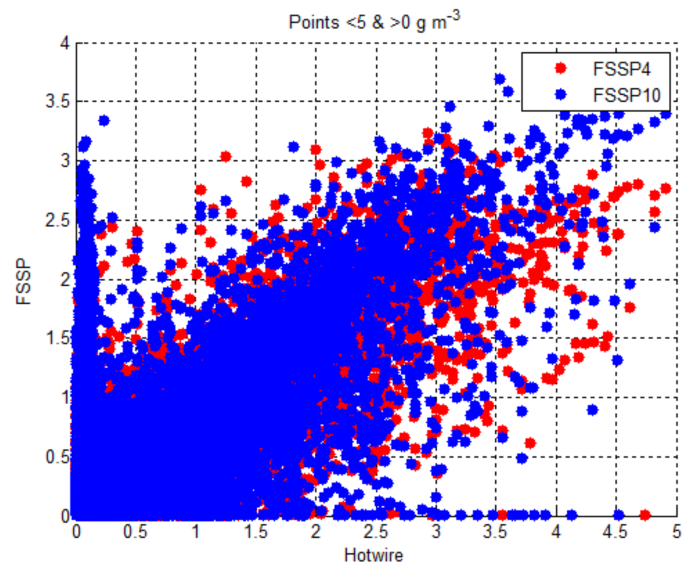

<5 gm^{-3}	FSSP4	FSSP10	Hotwire
FSSP4		0.956	0.794
FSSP10			0.745
>0 & <5 gm^{-3}	FSSP4	FSSP10	Hotwire
FSSP4		0.956	0.808
FSSP10			0.758

OAP data quality

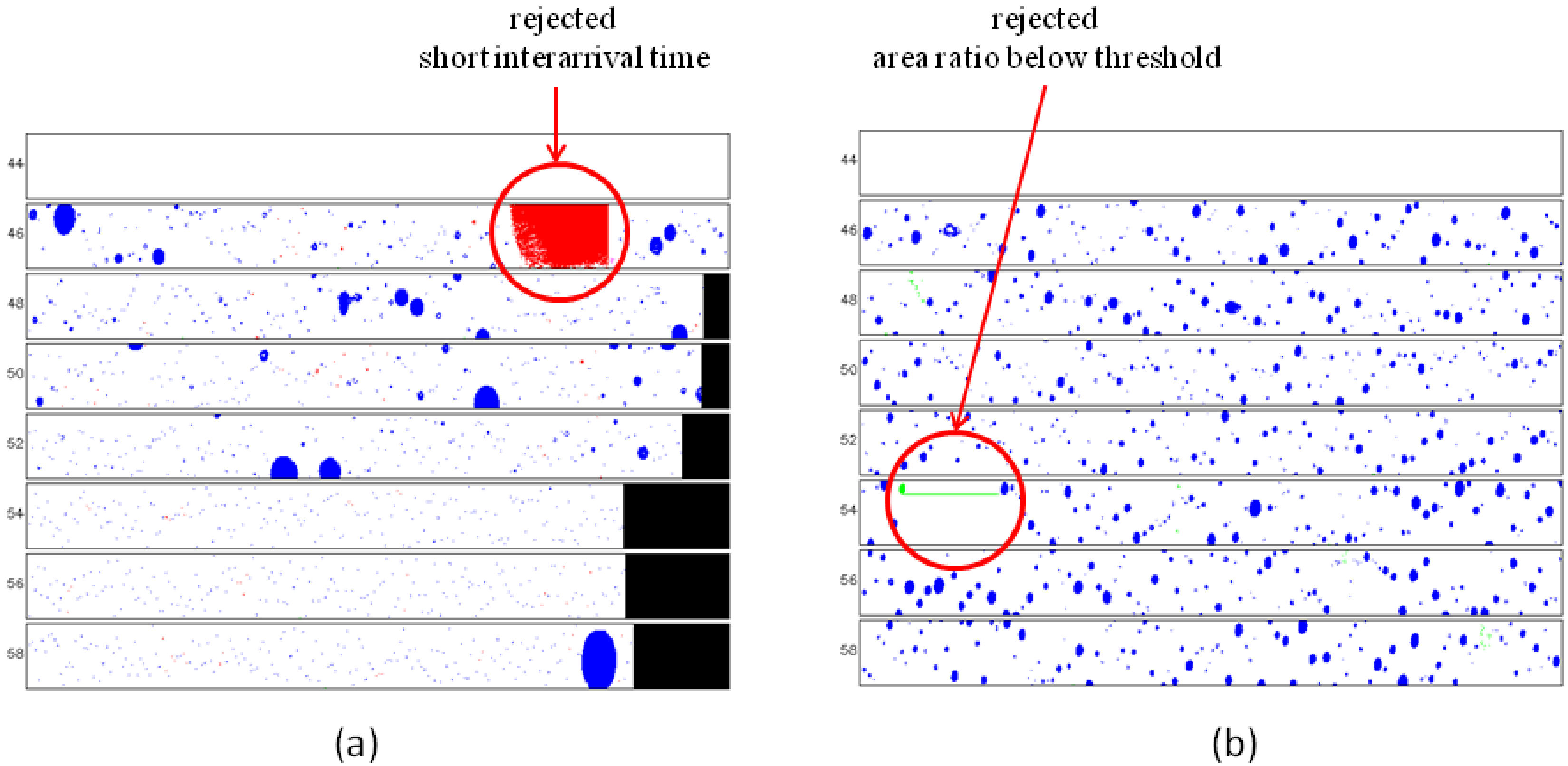

Processed CIP images (a) and PIP images (b) for 8 seconds of flight on 11 October 2011 (arf22) during 07:59:00 (one image strip for each second). The particles colored in blue are accepted and those that cross the array edges are reconstructed. The particles colored in red are rejected due to interarrival time being too short. The particles colored in green have an area ratio below the threshold value.

Literature review OAPs

- Cooper (1978): Developed particle inter-arrival time algorithm to remove shatterers in 2DC (modern CIP).
- Field et al. (2003): Revived interest in inter-arrival time algorithm as applied to fast FSSP data. Showed that previous FSSP measurements of small ice may have been misleading.
- Korolev high-speed video: Showed visual evidence that shattering produces hundreds to thousands of small ice fragments, some percentage of which will reach the sample volumes of scattering and imaging probes.
- Korolev new probe tip design based on icing tunnel and AIIE campaign: New probe tip design will reduce, but not eliminate effects of shattering.
- Jensen et al (2009), Baker et al. (2009), Lawson et al. (2010): Data from RICO, TC4, ISDAC and SPartICus field projects show that new (Korolev) probe tips reduce the amount of shattered particles, but not nearly as effectively as the inter-arrival time algorithm.

Sample volume in OAPs

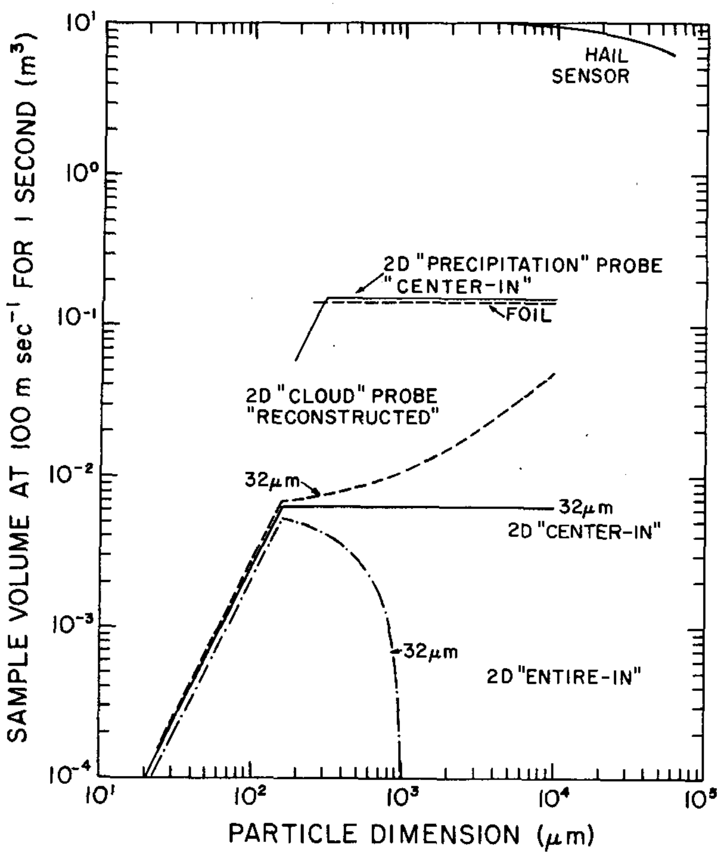

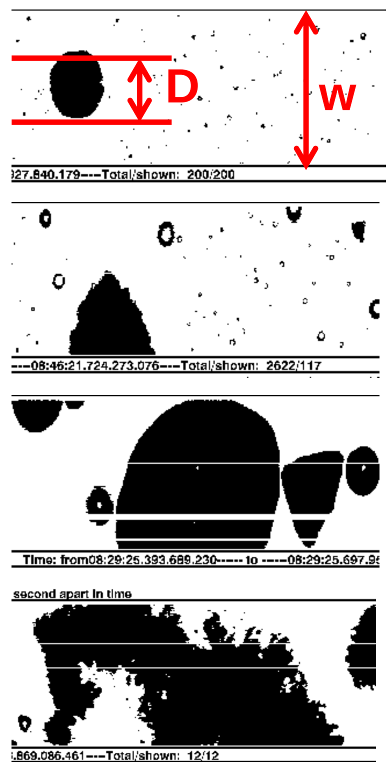

entire in D < w; sample area well defined

center in; particle obscuring one end element

center in; particle obscuring two end elements

aggregate of particles touching two end elements

Sampling volume swept out in 1 s of sampling at 100 m/s by 2-D probe for the entire-in, center-in and reconstructed techniques and for a 32 μm probe resolution (from Heymsfield and Parrish, 1978).

Image reconstruction

Geometry used to recompute size of particles:

a)particle obscuring one end element;
b)particle obscuring two end elements, with particle center inside of sensing area (left) and outside of sensing area (right);
c)aggregate of particles touching one end element (left) and both end elements (right)

(from Heymsfield and Parrish, 1978).

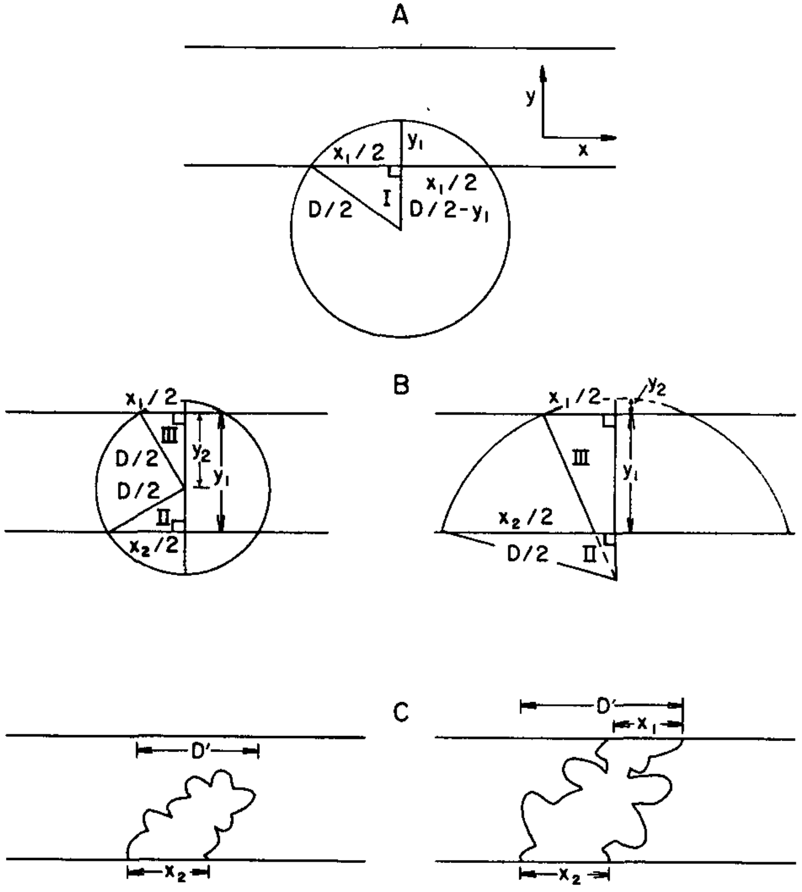

Fresnel diffraction

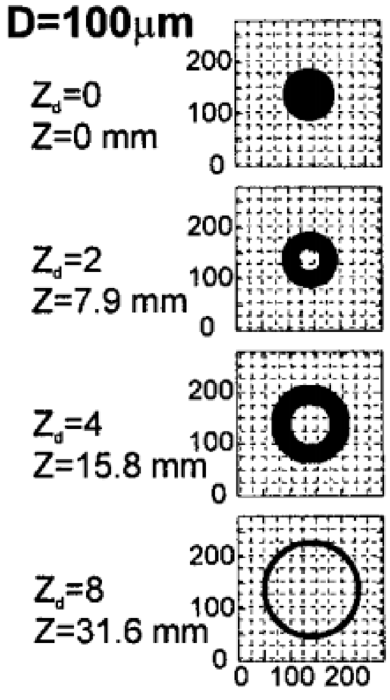

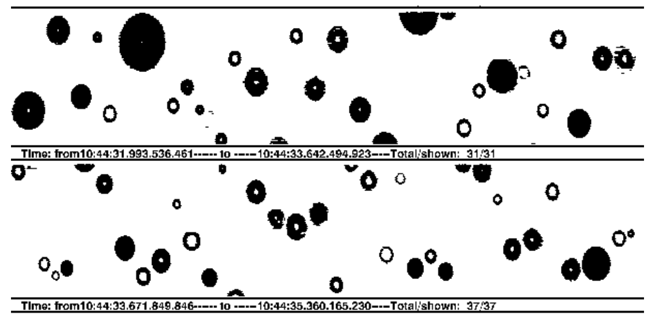

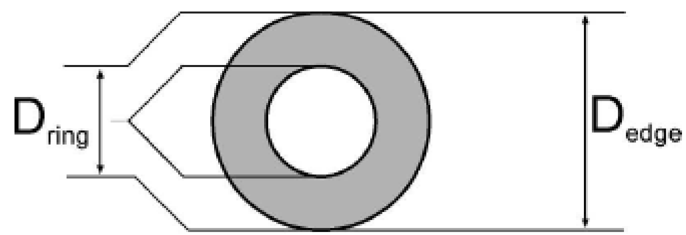

Calculated discrete images of 100 µm droplets at different distances from the object plane for a 25-µm resolution probe with a 50% intensity threshold. The original high resolution digital images are shown in the left with dashed lines denoting the imaginary photodiode grid

(from Korolev et al., 1998, correction described in Korolev 2007).

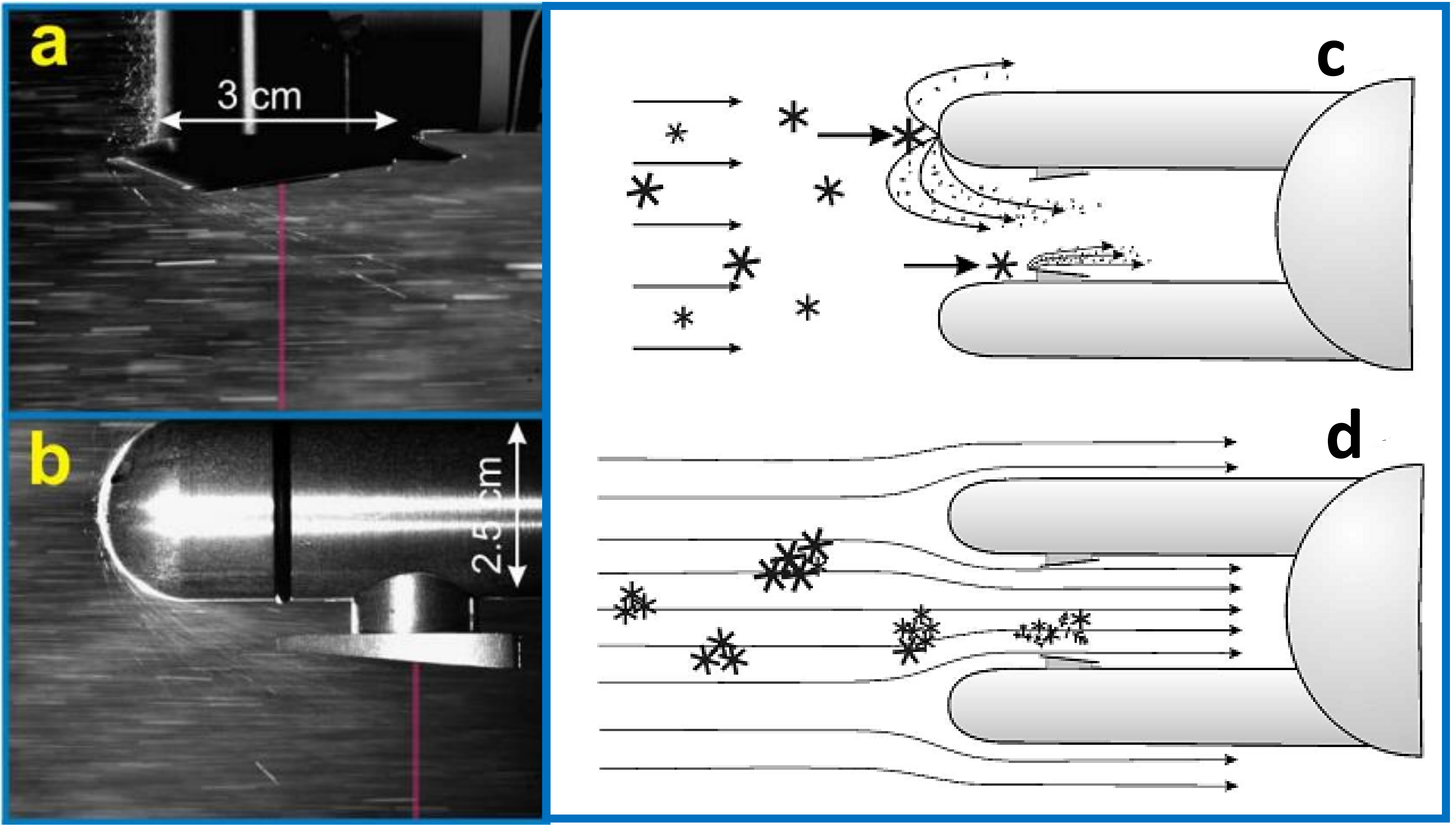

High speed video images of the trajectories of ice particles bouncing from the arm tips of CIP (a) and OAP-2DC (b). Frames are from high speed videos which were taken in ice wind tunnel at airspeed of 80m/s. Red line in (a) and (b) highlight the sample volumes of CIP (a) and OAP-2DC (b) probes, respectively. Particles unaffected by bouncing and shattering appear as horizontal lines (from Korolev et al 2010). Conceptual diagram of the mechanisms of the particle shattering during sampling by OAPs due to (c) the mechanical impact with probe parts upstream of the sample area and (d) the interaction with the aerodynamic field around the probe's housing (from Korolev and Isaac 2005).

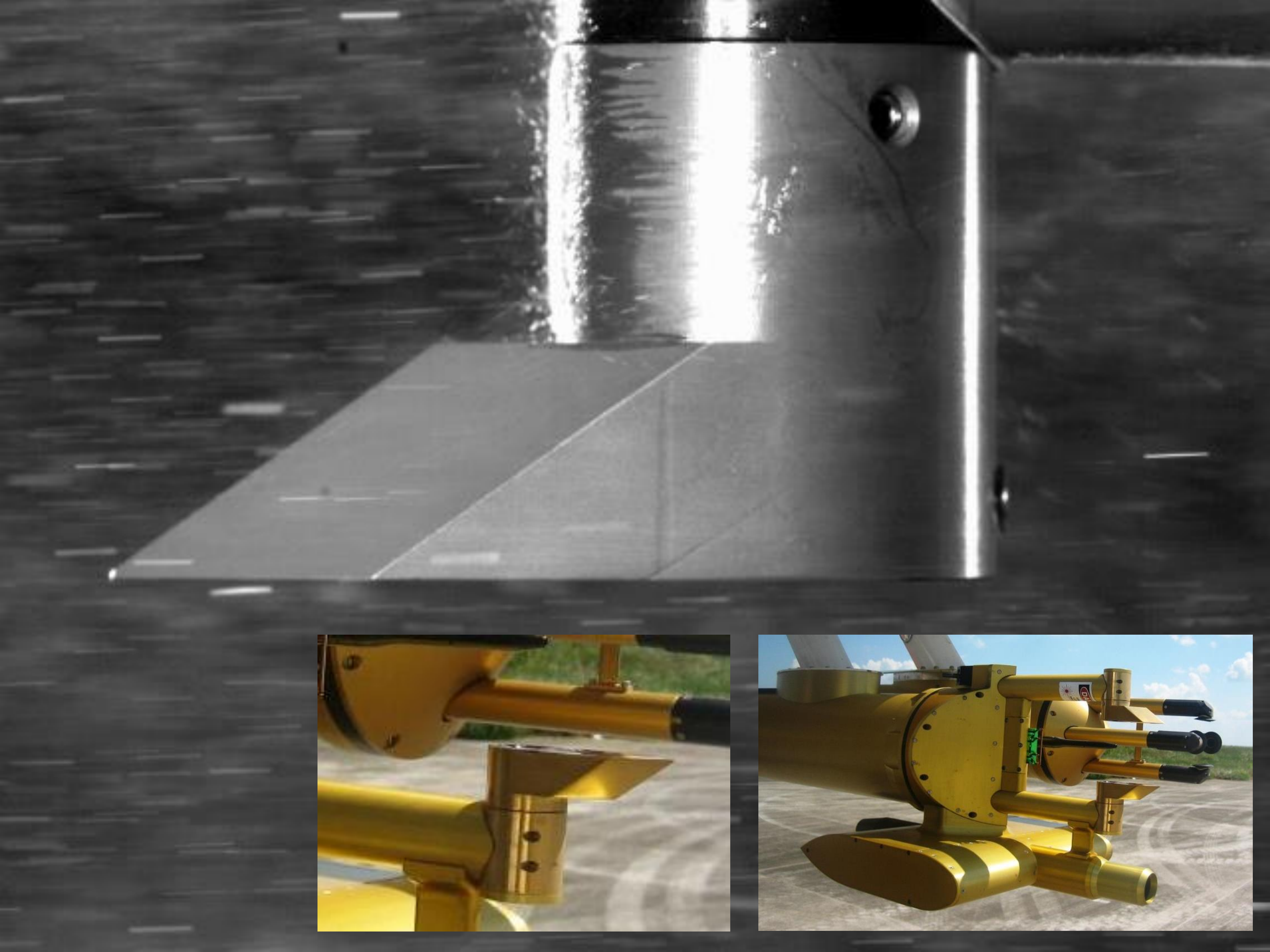

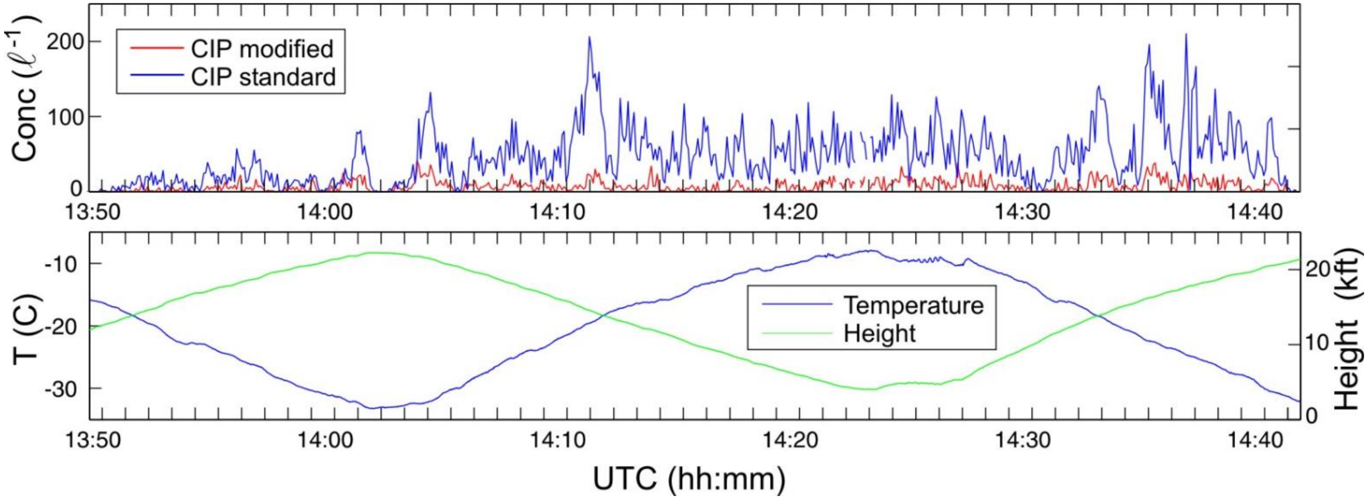

Korolev, A. V., E. F. Emery, J. W. Strapp, S. G. Cober, G. A. Isaac, M. Wasey, and D. Marcotte, 2010: Small ice particle observations in tropospheric clouds: fact or artifact?, Airborne Icing Instrumentation Evaluation Experiment, *B. Am. Meteor. Soc.*, 92, 967–973.

A summary of our current knowledge about shattering artifacts:

1. After impact with a solid surface, an ice particle may shatter into small fragments. The number of fragments that intersect the probe's sample volume may reach a few hundred per shattered particle
2. At aircraft speeds, the size of particle fragments has been observed to be as small as 10 μm
3. Shattered particles often form a cluster of closely spaced fragments. The dimension of the clusters depends of the shape of the surface, angle of impact, particle properties and airspeed.
4. Shattering occurs mostly in mixed phase and ice clouds, depends on particle size and the number concentration may vary from a few times, when particles are less than one millimeter, to two orders of magnitude, when the maximum size of particles exceeds five millimeters.
5. Instrumentations PIs have attempted to minimize these artifacts by modifying the probe inlets, and by applying interarrival time algorithms. Using these methods the effects of shattering can be significantly reduced.

Area ratio $AR = \frac{A_p}{\pi r^2}$

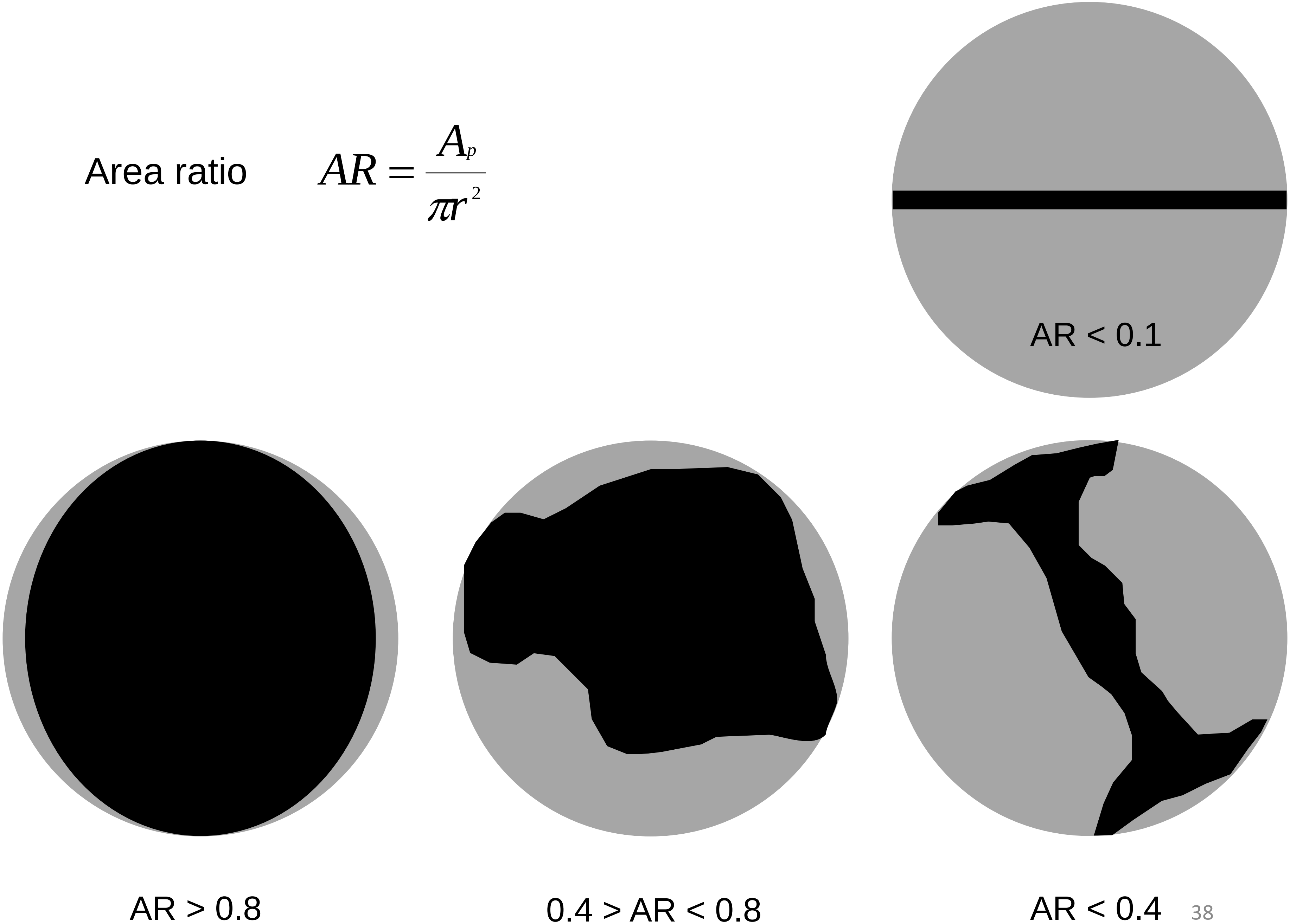

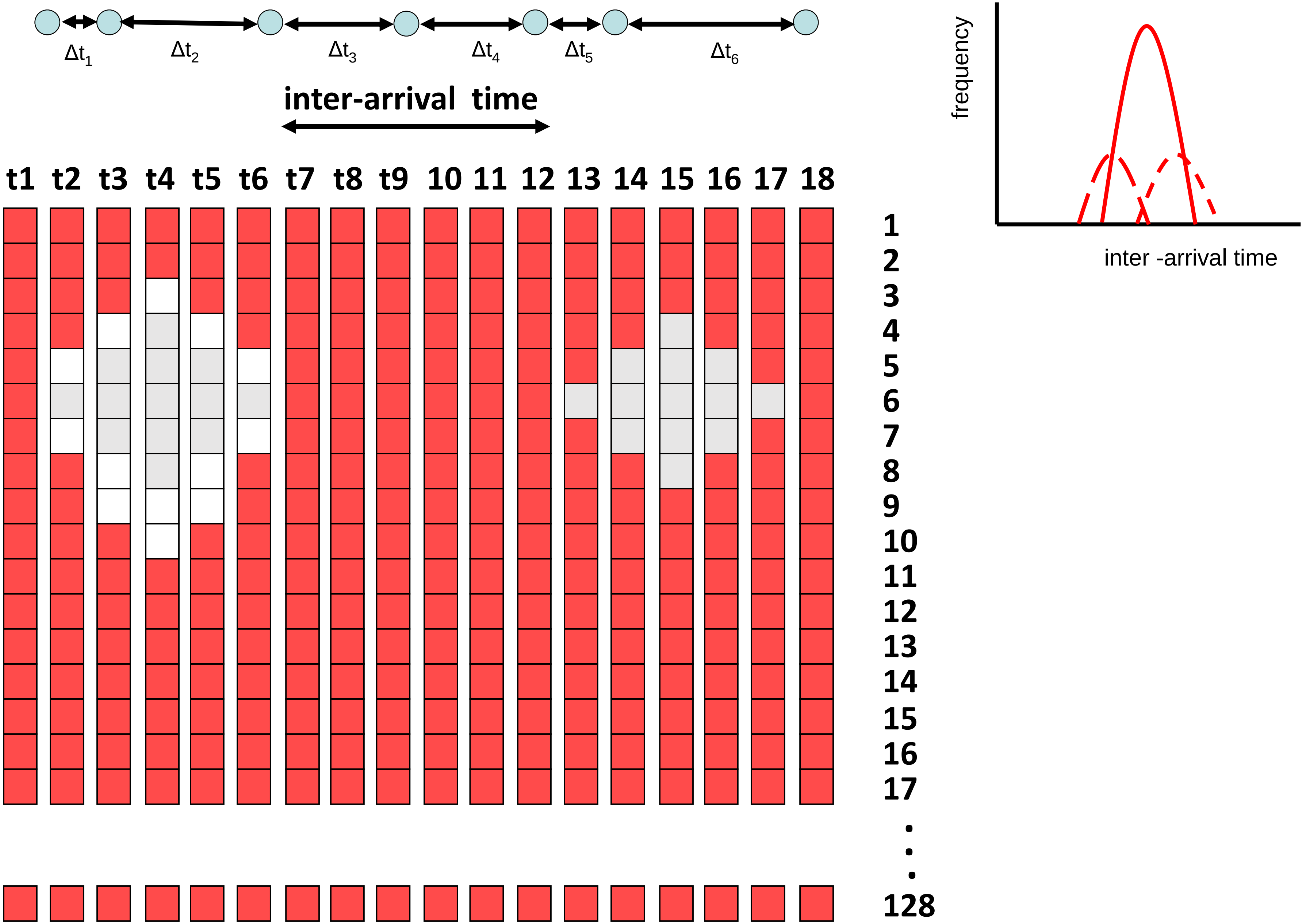

Δt1
Δt2
Δt3
Δt4
Δt5
Δt6
inter-arrival time
t1 t2 t3 t4 t5 t6 t7 t8 t9 10 11 12 13 14 15 16 17 18
1
2
3
4
5
6
7
8
9
10
11
12
13
14
15
16
17
128
frequency
inter -arrival time

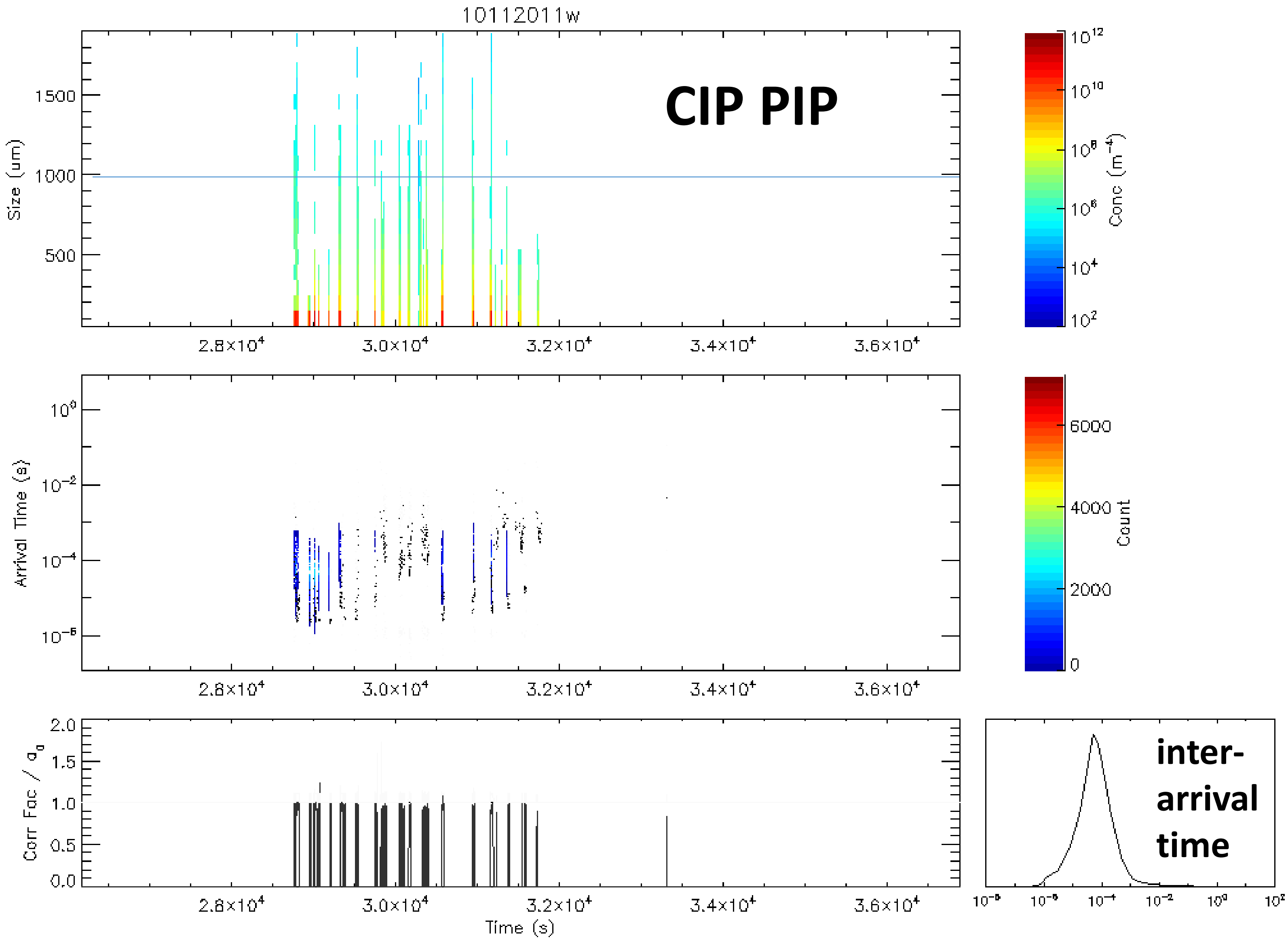

The top panel shows the size distribution of the CIP for 11 October 2011 (arf22). The middle panel shows a frequency plot of the CIP particle arrival time. The bottom panel shows the correction factor (left) and the distribution of interarrival time (right).

2DS inter-arrival times

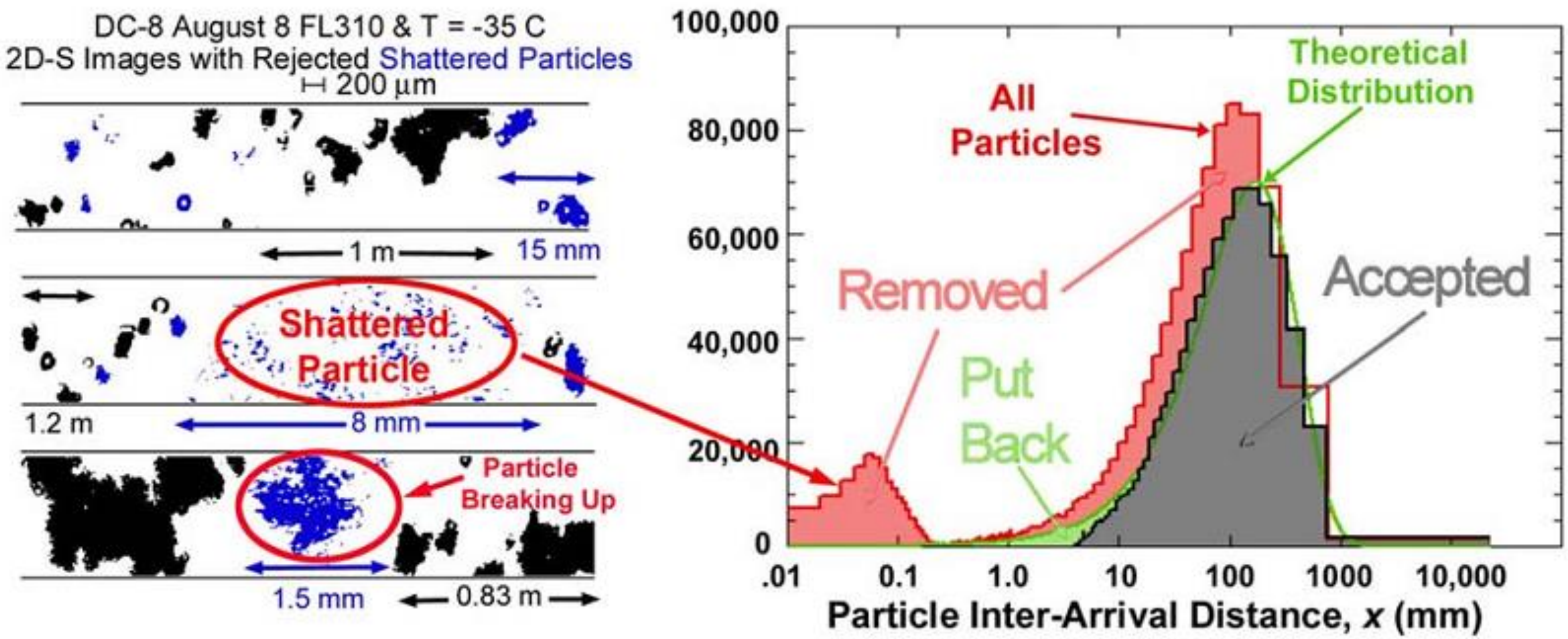

Example of (left) 2D-S images with particles in blue identified as artifacts, and (right) plot of particle events versus interarrival distance showing (in red) the inter-particle distances before removing shatterers, (in black-grey) the remaining ("Accepted") particles' inter-particle distances after "Removing" shatterers, and (in green) an exponential distribution with the same mean as the after-shattering removal distribution, for comparison (labeled "Theoretical Distribution").

Removal of 2D-S artifacts - shatterers

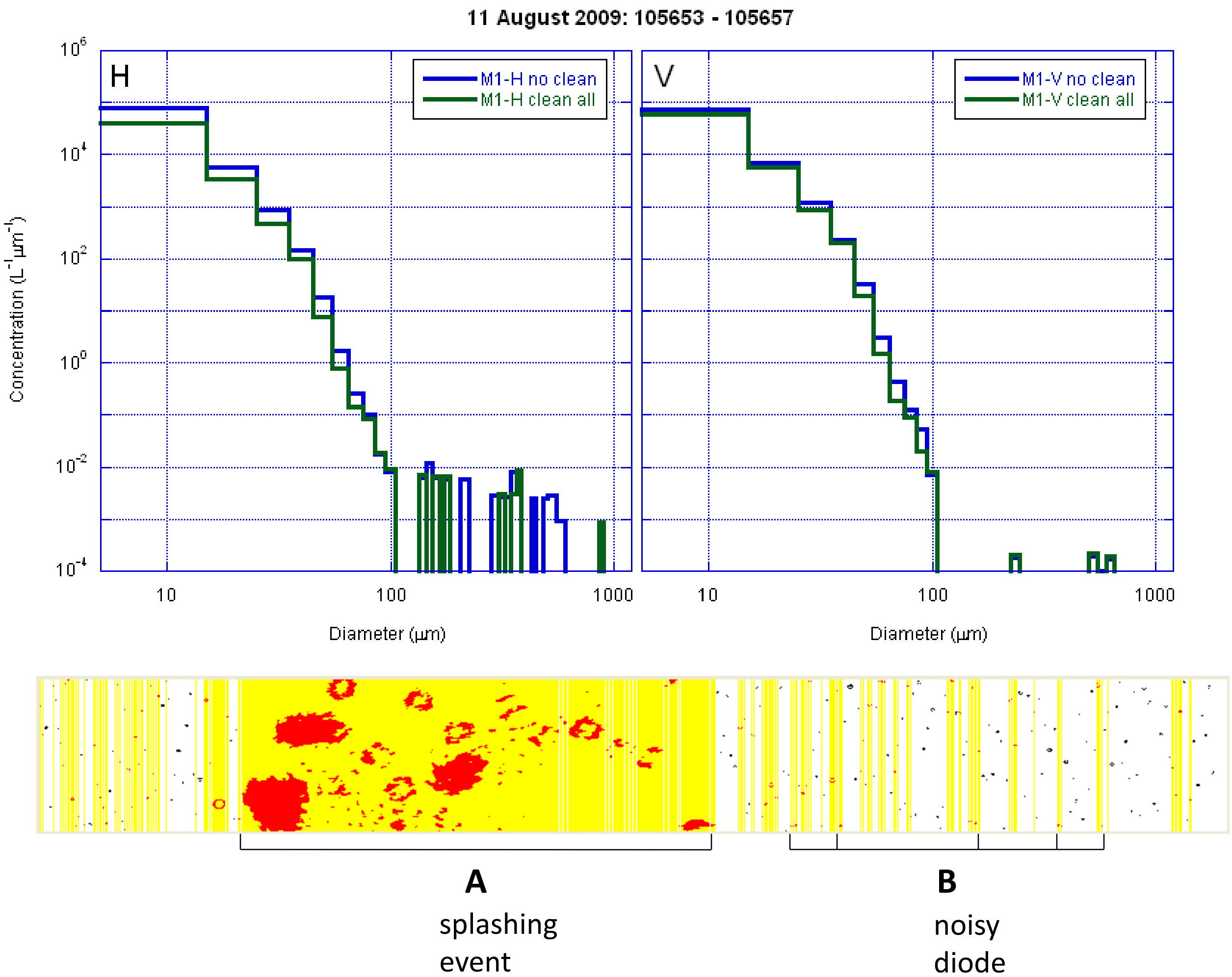

Example of 2D-S splashing event (A) and noisy diode data (B) intermixed with “accepted” particle data for the vertical channel on 11 August 2009 (Saudi Arabia). The yellow highlighting identifies the “rejected” particles.

Kucera, P.A., D. Axisa, R.P. Burger, D.R. Collins, R. Li, M. Chapman, R. Posada, T.W. Krauss and A.S. Ghulam, 2010: Features of the Weather Modification Assessment Project in the southwest Region of Saudi Arabia. *J. Wea. Modification*, 42, 78-103.

Removal of 2D-S artifacts – noisy diodes

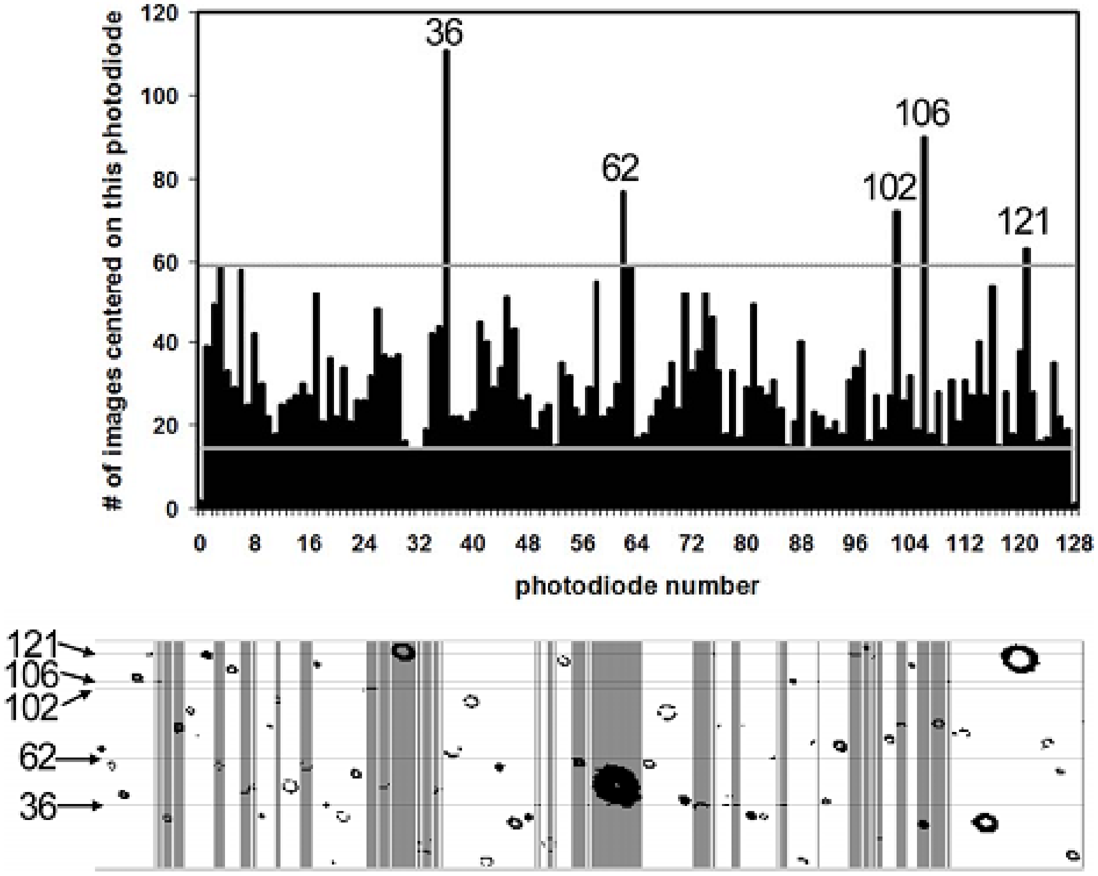

Example of noisy diode data intermixed with good particle data. The images highlighted are rejected. Images centered on diodes determined to be bad (too noisy) by the criteria and exemplified in the particle center location distribution shown above.

Two 2D-S probes, one with Standard Tips and one with Modified Tips, were installed side-by-side for a flight on the SPEC Learjet during NASA SPARTICUS

from Lawson ppt MACPEX

2D-S Images with Standard Probe Tips

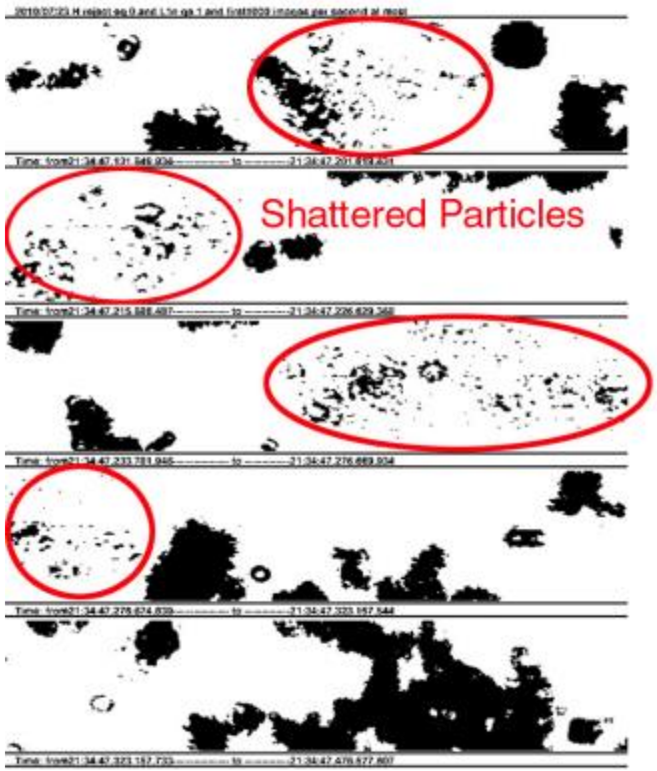

2D-S Images with Modified Probe Tips

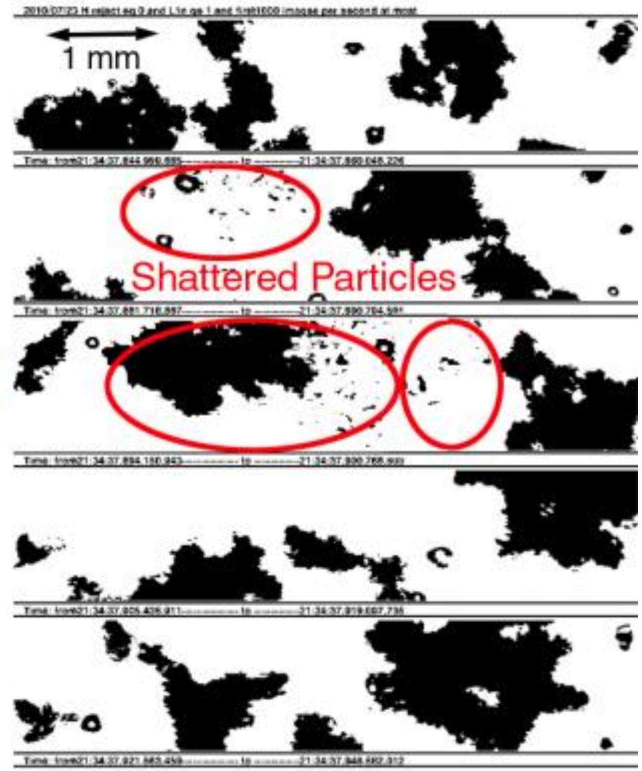

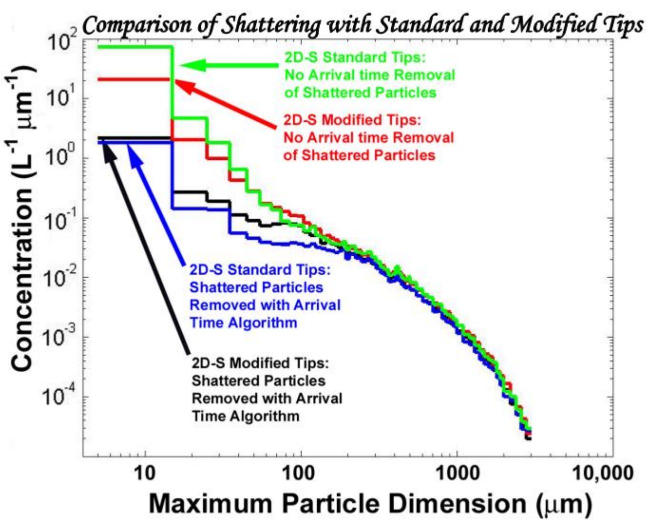

from Lawson ppt MACPEX

Derivation of bulk parameters

Number concentration (cm^{-3}) $$C_T = \sum_{i=1}^{m} c_i = \sum_{i=1}^{m} \frac{n_i}{SV_i}$$

used for PCASP, CCN, CAS, CDP and FSSP

where
C_T = total concentration (units = # /cm^{-3})
c_i = number concentration in channel i
n_i = number of particles accumulated in channel i
m = total number of size channels
SV = Sample Volume = (Sample Area)(airspeed)(sample time)

Effective Radius (μm) $$R_e = \frac{3\sum_{i=1}^{m} c_i d_i^3}{4\sum_{i=1}^{m} c_i d_i^2}$$

Liquid water content (gm^{-3}) $$LWC = \frac{\pi\rho_w}{6}\sum_{i=1}^{m} c_i d_i^3$$

Effective density relations

TABLE 1. Effective density relations.

Habit	Two-parameter coefficients habit code	$\rho_e = k(A_r)^n$ k	n	r^2	A_r	Range
Columns (theory)	C1e-C1f	$0.97\rho_b$	2.10	1.00	0.05	0.64
Rosettes (theory)	C2a					
No. of bullets		($\rho_b = 0.81$ g cm^{-3})				
1		0.60	1.94	0.99	0.22	0.98
2		0.66	2.11	0.99	0.11	0.55
3		0.54	2.11	0.99	0.16	0.68
4		0.47	2.16	0.99	0.20	0.87
5		0.49	2.16	0.99	0.22	0.87
6		0.49	2.25	0.99	0.26	0.99
7		0.50	2.35	1.00	0.29	0.99
8		0.52	2.52	0.99	0.32	1.00
Side planes, S1–S3, (Observatory)		0.35	2.34	0.79	0.18	0.88
Planar crystals						
Wind tunnel	P1a-P1b-P1d	0.084	2.38	0.97		<0.79
(Takahashi et al. 1991)		11.96	22.64	0.48		≥0.79
Sfc. observations	Many types	0.102	3.29	0.86		<0.81
(Heymsfield and Kajikawa 1987)						
$A_r = 0.83$	Thick plates	$\rho_e = 0.043\ d^{-[illegible]}$				
Aggregates						
Magono and Nakamura (1965)	Planar crystals	0.010	1.50		0.28	1.0
Kajikawa (1982)	2–6 planar crystals	0.015	1.50		0.13	0.77
Agg. side planes (Sfc.)	S1–S3	0.18	1.52	0.97	0.21	0.65
CPI observations (ARM)	Rosettes	0.16	1.48	0.99	0.16	0.56

Aggregate ρ_e vs D relationships
$\rho_e = \chi D^{\kappa}$

Aggregate study	Component crystals	χ	κ
Magono and Nakamura (1965)	Planar crystals	0.0142	−1.43
Kajikawa (1982)	2–6 planar crystals	0.00089	−1.23
Side planes (Obs.)	S1–S3	0.0061	−0.92
CPI rosettes	C2a	0.0035	−0.96

Aggregate hybrid approach
$\rho_e = kA_r^n D^{\alpha}$

k	n	α
0.015	1.5	−1.0

$\rho_e = k(A_r)^n D^{\alpha}$

CIP PIP processing procedure

The CIP and PIP processing attempts to correct the cloud probe size distribution that is used for the calculation of other parameters. To apply this correction we proceed with the following method (from Field et al. 2006):

- Reject particles with area ratio <0.1, to remove “streakers” (long, thin images caused by splash or shatter products traveling slower than the true airspeed through the sample volume) and image frames containing multiple particles.
- Reject particles associated with corrupted timelines or timelines indicating all 1 or 0 s.
- Eliminate, through software processing, all of the particles with interarrival times less than the ‘long’ mode. Do not eliminate particle interarrival time from integrated probe-elapsed time.
- Eliminate the invalid first particle in a train of fragments by removing the particle that precedes particles removed for having a short interarrival time. Do not eliminate particle interarrival time from integrated probe-elapsed time.
- Multiply the particle concentrations within all size bins by the correction factor derived from the Poisson function.

CIP PIP processing options

The processing options for the CIP and PIP are as follows:

- All-in: Rejects all particles that touch the edge of the array, and makes the appropriate adjustment to the sample volume.
- PBP: Writes a particle-by-particle file in addition to the .dat file.
- Stuck bit: Applies an algorithm to check for dead/stuck bits and makes a correction using neighboring array elements.
- Variable time rejection: Turn on shattering correction (Field et al. 2006).
- Water: Accepts only round-ish particles up to 6mm, accepts particles with high area ratio criterion (>0.6) and makes a size correction based on Korolev's poisson-spot reconstruction (Korolev 2007).

The processing options for ice particle mass-size parameterization are as follows:

- CRYSTAL: k = 0.0116, n = 0, α = −0.95 (default for ‘ice’)
- Brown/Francis: k = 0.00561, n = 0, α = −1.1
- TRMM: k = 0.0700, n = 1.5, α = −0.5
- Water: k = 1.0, n = 0, α = 0 (default for ‘water’)
- Other: k = specify, n = specify, α = specify

$\rho_e = k(A_r)^n D^\alpha$

$m = g_0 D^{g_1}$

where $g_0 = 0.0061$, $g_1 = 2.0$

arf22 - 20111011

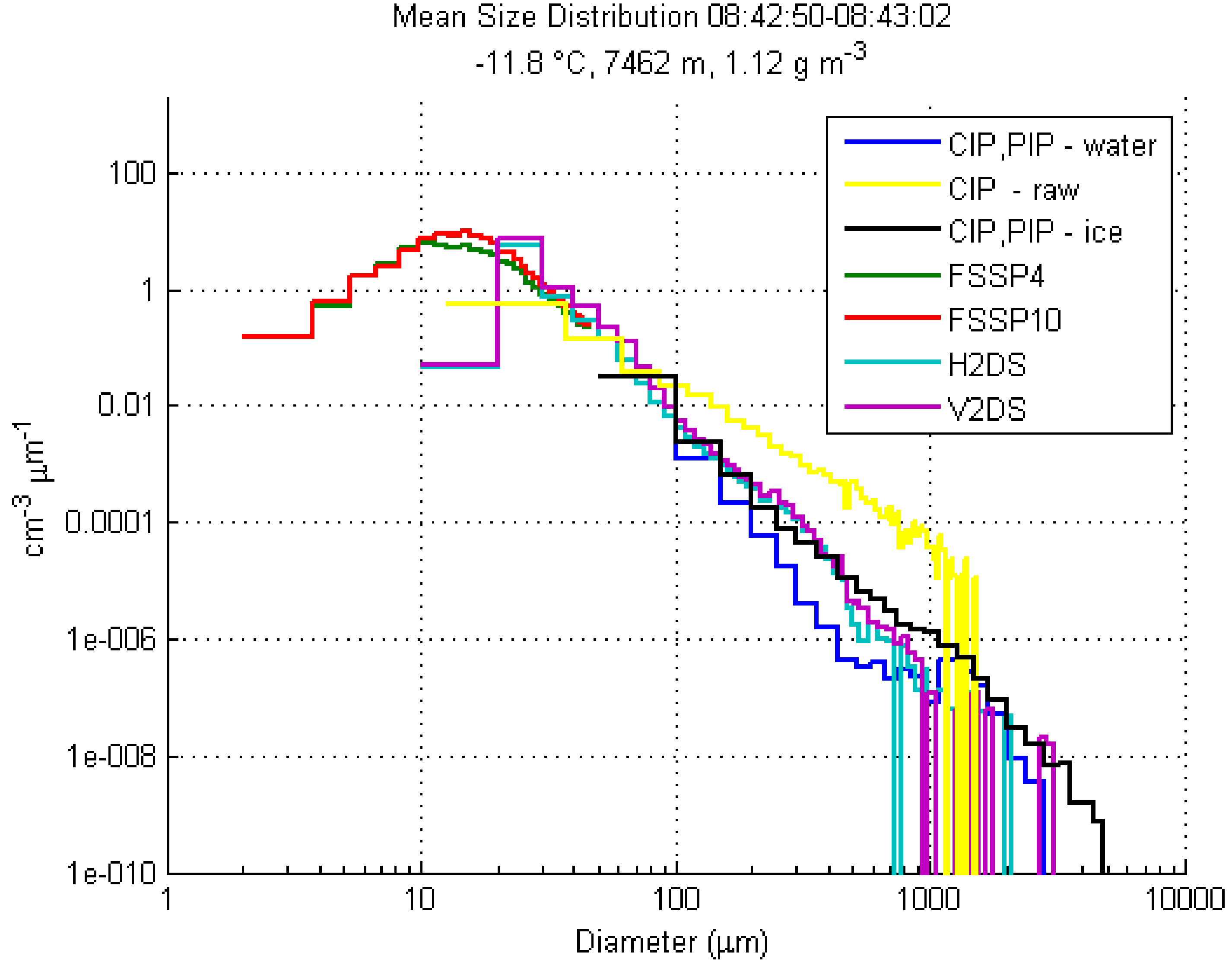

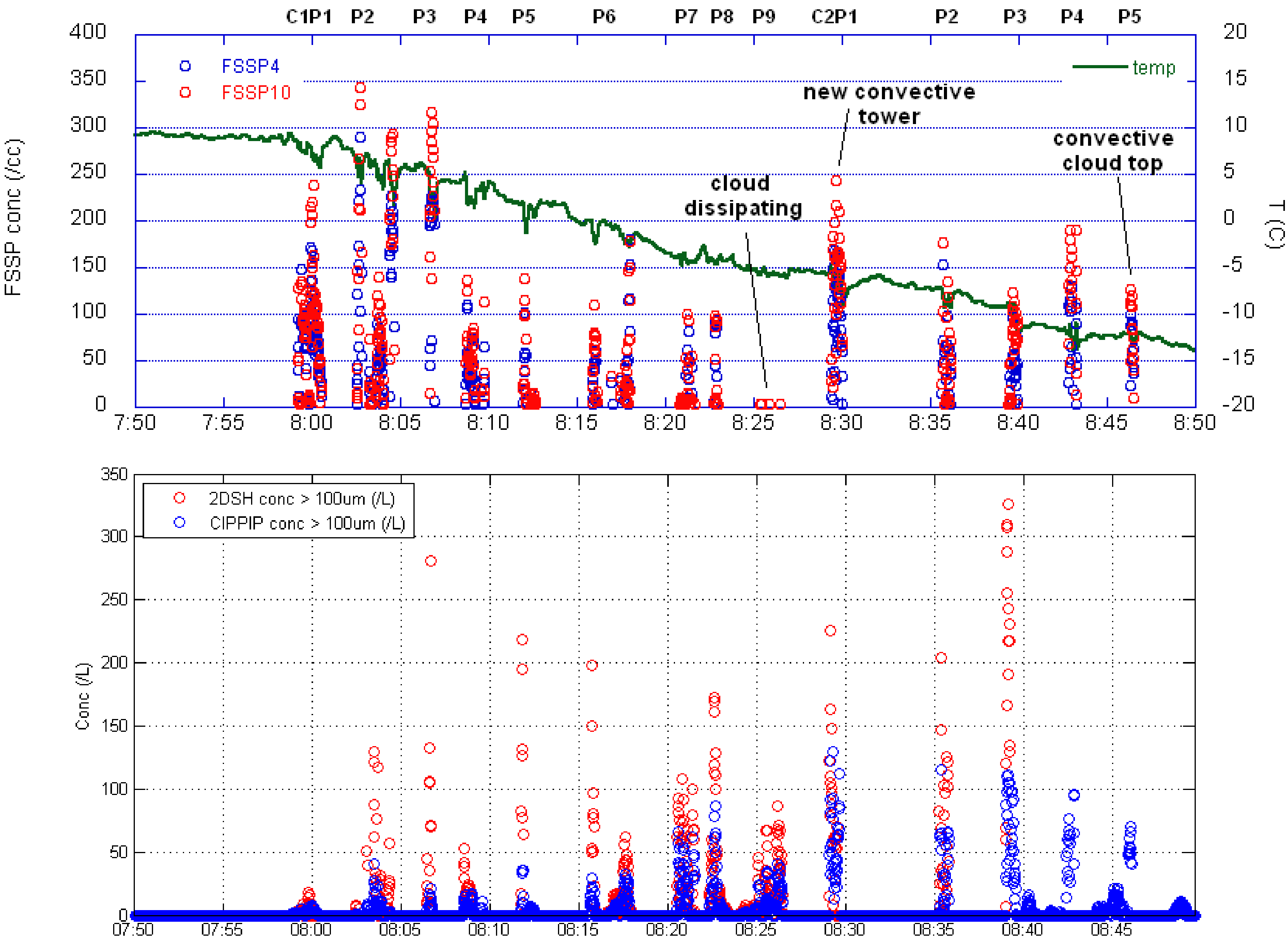
C1P1
P2
P3
P4
P5
P6
P7
P8
P9
C2P1
P2
P3
P4
P5
FSSP4
FSSP10
temp
new convective tower
convective cloud top
cloud dissipating
FSSP conc (/cc)
T (C)
7:50
7:55
8:00
8:05
8:10
8:15
8:20
8:25
8:30
8:35
8:40
8:45
8:50
2DSH conc > 100um (/L)
CIPPIP conc > 100um (/L)
Conc (/L)

Advertisement

Olympics of Cloud Physics coming to Pune in 2020

Indian Institute of Tropical Meteorology (IITM)

and

International Commission on Clouds and Precipitation http://www.iccp-iamas.org/

Will be hosting

International Conference on Clouds and Precipitation ICCP 2020

Thank you